RESEARCH ARTICLE

Figures and figure supplements

Cortex cis-regulatory switches establish scale colour identity and pattern diversity in *Heliconius*

Luca Livraghi *et al*

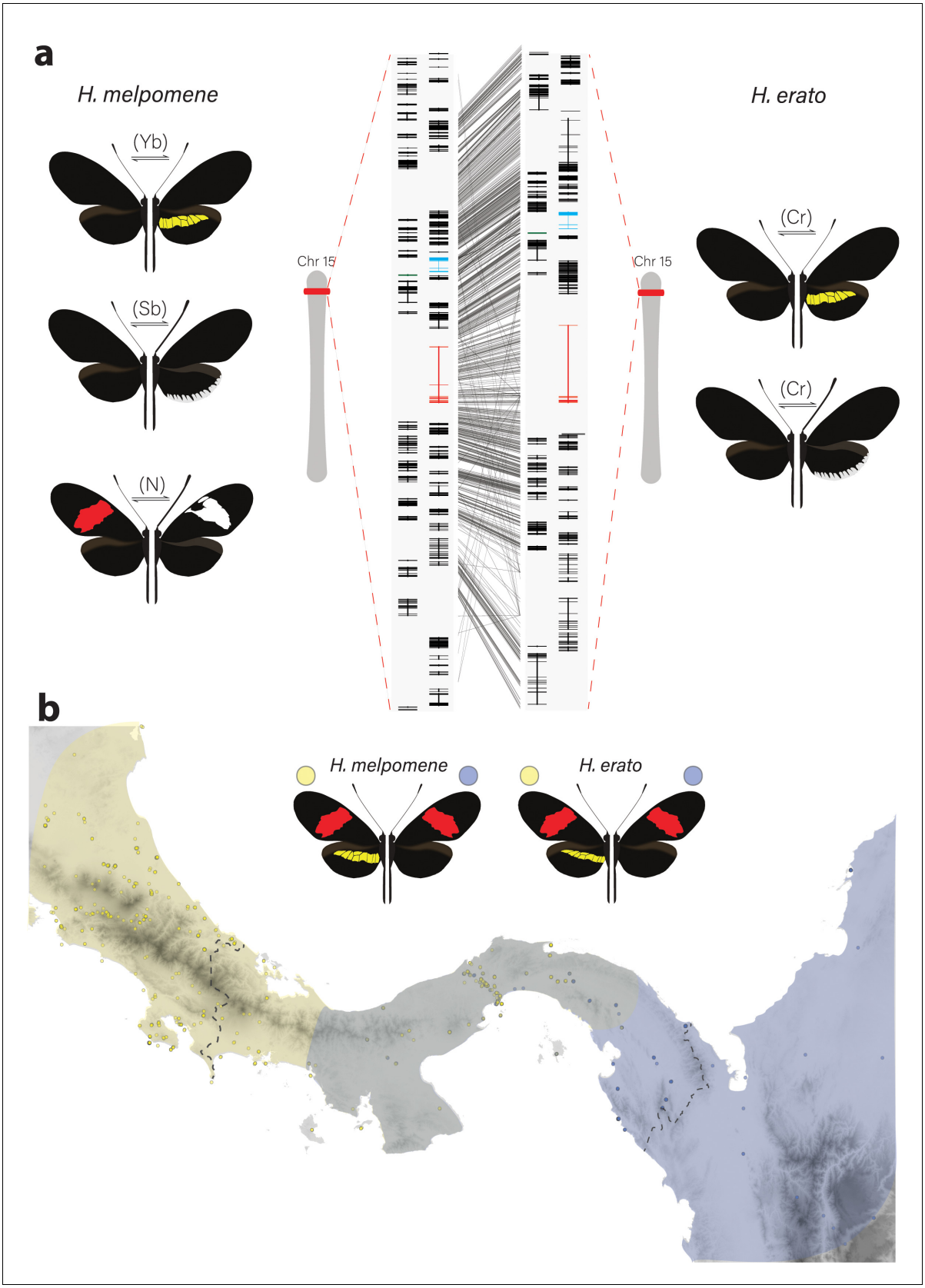

Figure 1. Phenotypic switches of yellow and white colour pattern elements are controlled by homologous loci in *Heliconius* species. (**a**) Homologous loci in both *H. erato* and *H. melpomene* are associated with variation in yellow and white patterns between morphs. In *H. melpomene*, three tightly

Figure 1 continued on next page

Figure 1 continued

linked genetic elements located at chromosome 15 have been identified that control variation for the hindwing yellow bar, white margin elements, and forewing band (Yb, Sb, and N, respectively), while in *H. erato*, variation has been mapped to one element (Cr). The gene *cortex* is highlighted in red, *dome/wash* in blue, and *dome-trunc* in green. Alignments between the two co-mimetic species at the locus is shown (grey lines, 75% alignment identity). Gene models from assemblies of *H. melpomene* (left) and *H. erato* (right) are shown for the loci spanning the associated intervals controlling the phenotypic switches highlighted. Horizontal bars indicate exons, vertical bars introns. (**b**) Focal co-mimetic morphs of *H. erato* and *H. melpomene* used in this study, differing in the presence of a hindwing yellow bar, and their ranges across Central America are shown. Yellow: yellow banded morphs, blue: black hindwing morphs, grey: range overlap. Each dot represents a sampled location (data from ***Rosser et al., 2012***). Country borders are indicated by dotted lines.

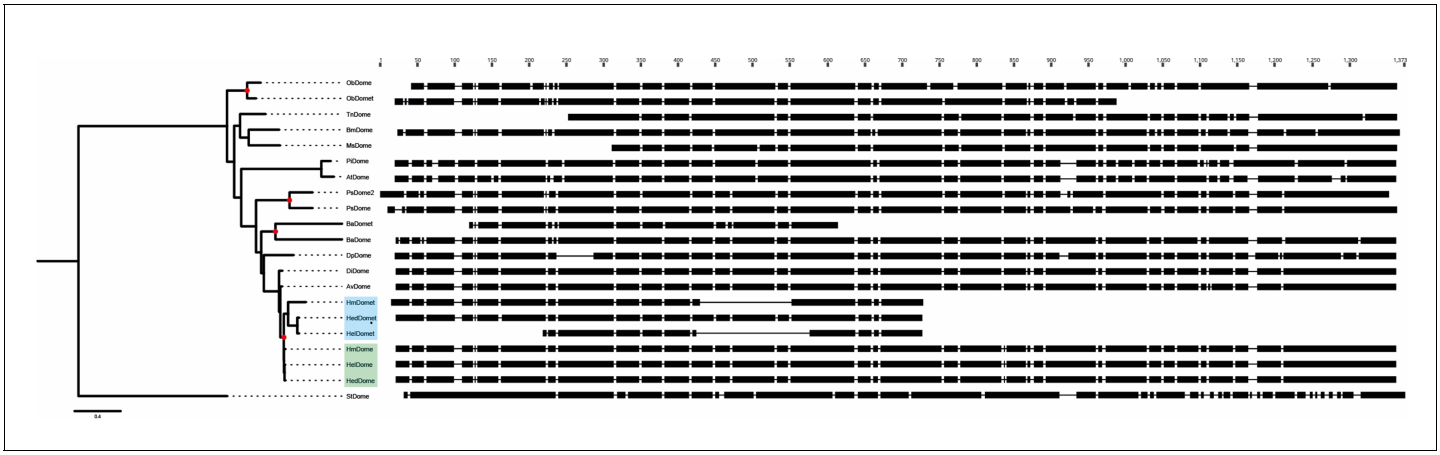

Figure 1—figure supplement 1. Maximum-likelihood tree based on lepidopteran *dome* amino acid sequences. The *Heliconius* duplications are highlighted in blue (*dome-t*) and green (*dome*). Putative duplication events are shown with a red circle. Protein alignments are shown alongside each species, illustrating several C-terminal truncation events in the duplicated sequences. Protein alignments indicate that in both *H. erato* and *H. melpomene*, *dome-trunc* maintains only the N-terminal half of the gene, suggesting *dome-trunc* is undergoing pseudogenisation. *H. melpomene* (Hm), *H.erato demophoon* (Hed), *Operophtera brumata* (Ob), *Trichoplusia ni* (Tn), *Bombyx mori* (Bm), *Manduca sexta* (Ms), *Plodia interpunctella* (Pi), *Amyeolis transitella* (At), *Phoebis sennae* (Ps), *Bicyclus anynana* (Ba), *Danaus plexippus* (Dp), *Dryas iulia* (Di), *Agraulis vanillae* (Av), and *Heliconius erato lativitta* (Hel). All lepidoptera sequences were extracted from the assemblies deposited on lepbase.org. As a trichopteran outgroup, we used a recently published Pacbio assembly of *Stenopsyche tienmushanensis* (St) (***Luo et al., 2018***).

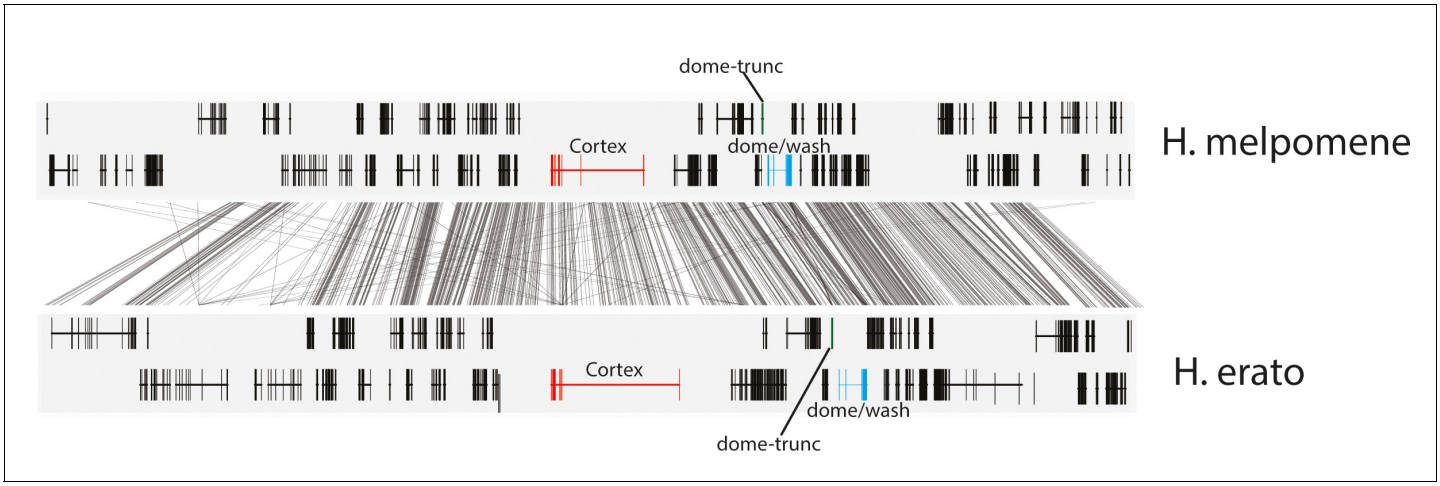

Figure 1—figure supplement 2. Annotation of the genes present in the 47 gene interval previously shown to be associated with colour pattern differences in *Heliconius*. The positions of *cortex* (red), *dome-trunc* (green), and *dome/wash* are highlighted. Alignments between the two species at the locus is shown (grey lines, 75% alignment identity). Gene models from assemblies of *H. melpomene* (top) and *H. erato* (bottom) are shown for the loci spanning the associated intervals controlling the phenotypic switches highlighted. Horizontal bars indicate exons, and vertical bars indicate introns.

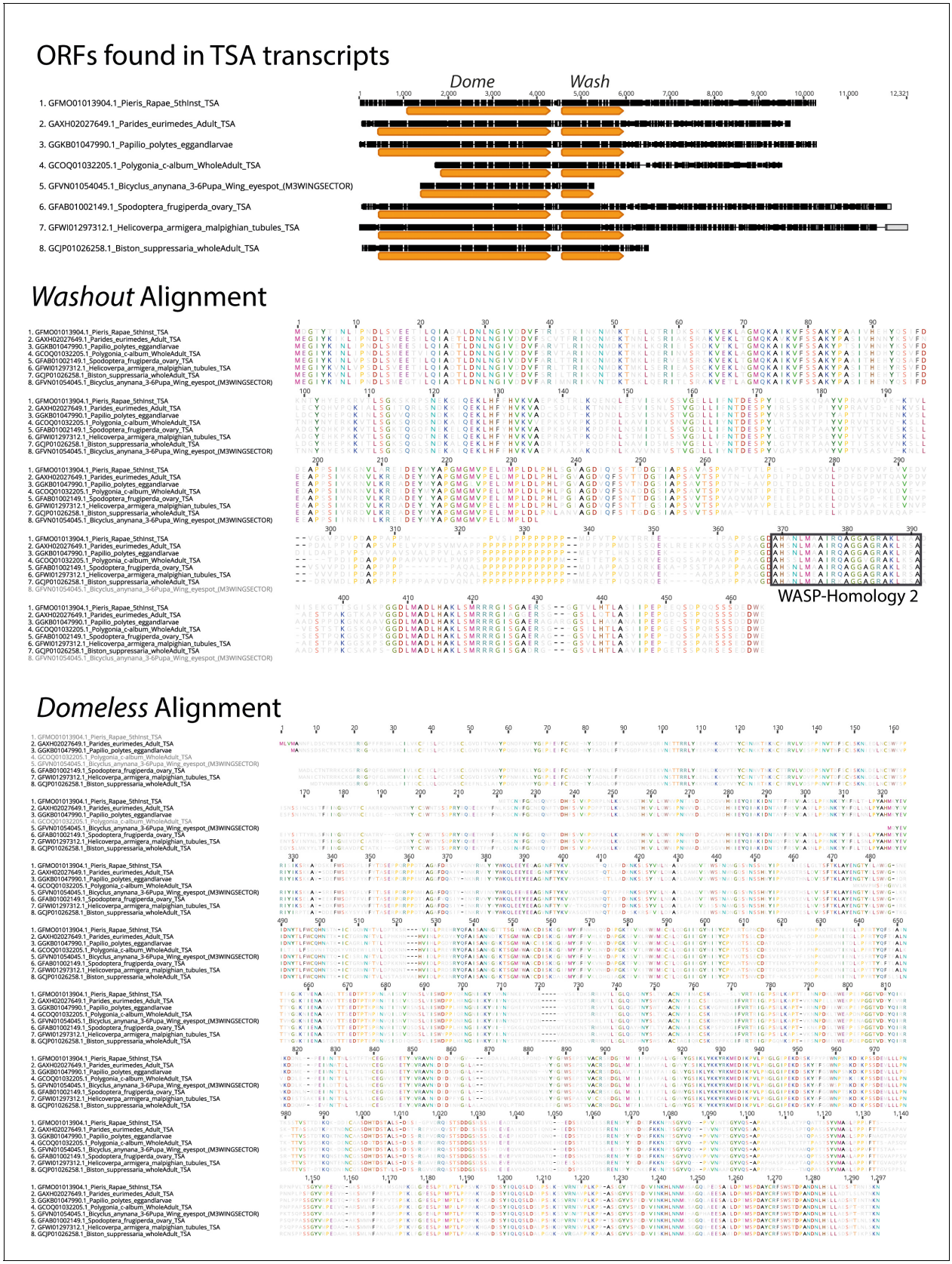

Figure 1—figure supplement 3. To examine the conservation of *dome/wash* bi-cistronic transcription in the Lepidoptera, we performed BLASTn searches using the previously annotated *dome* transcripts from the *H. melpomene* genome (Hmel2) found on Lepbase (***Challi et al., 2016***), against the

Figure 1—figure supplement 3 continued on next page

Figure 1—figure supplement 3 continued

Transcription Shotgun Assembly (TSA) sequence archive on NCBI. We recovered several assembled transcripts containing both the *dome* and *wash* ORFs in various divergent lepidoptera. The positions of *dome* and *wash* ORFs are shown (arrows blocks in TSA transcript) as well as the encoded Wash and Dome proteins below.

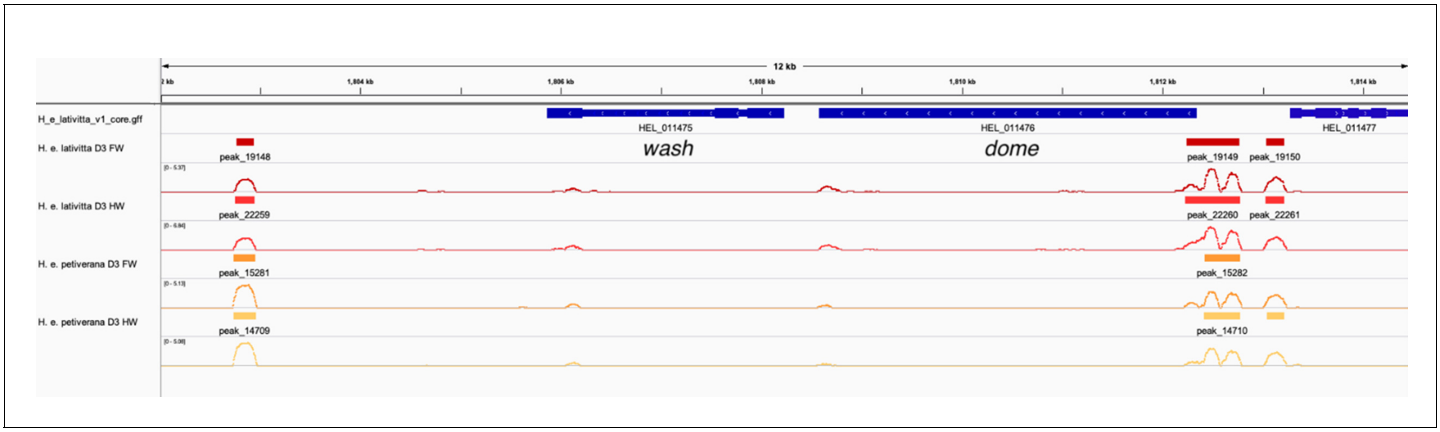

Figure 1—figure supplement 4. ATAC-sequencing analysis supports *dome/wash* bi-cistronic transcription in *Heliconius erato*. We explored whether *dome/wash* share a promoter by analysing published ATAC-sequencing data from ***Lewis et al., 2019***. We analysed samples corresponding to the forewings and hindwings of day three pupa of *H. e. lativitta* and *H. e. petiverana*. Peaks were called using Genrich (http://github.com/jsh58/Genrich/ (***Gaspar, 2021***), using the parameter -j (ATAC-seq mode) with a cutoff of $q < 0.05$ (q = FDR adjusted p-value). Peaks were visualised in IGV. Coloured blocks correspond to significant peaks and lines represent -log(q). Peaks, indicating *cis*-regulatory activity, were observed upstream of *dome* for all samples, whereas no peaks were present upstream of the start of *wash*, indicating a shared promoter for *dome/wash*.

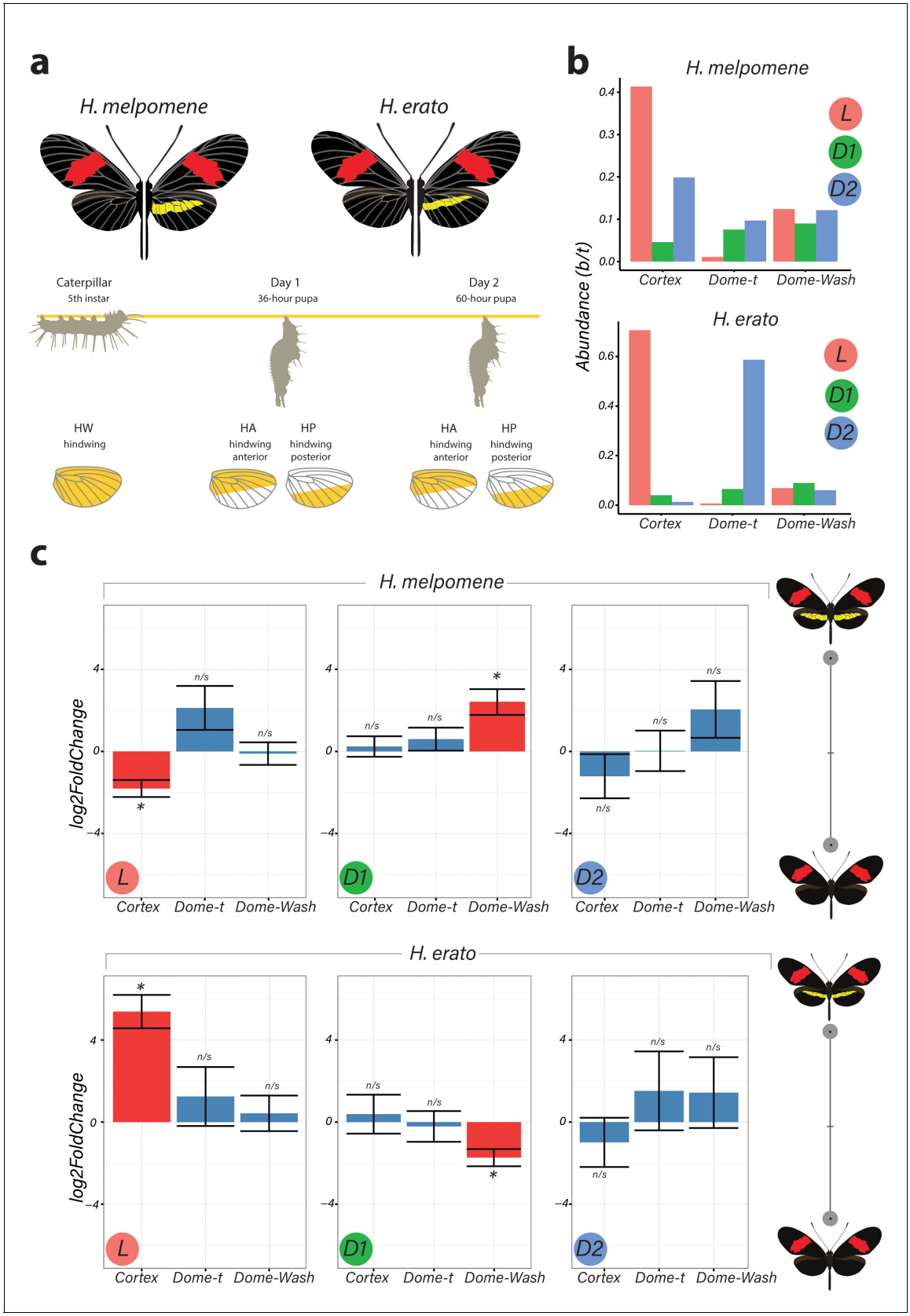

Figure 2. Differential expression of genes at Chromosome 15 implicate *cortex* as most likely candidate driving yellow bar differences. (**a**) Hindwing tissue from co-mimetic morphs of *H. melpomene* and *H. erato* were collected at three developmental stages fifth-instar caterpillar, Day 1 Pupae

Figure 2 continued on next page

Figure 2 continued

(36hAPF) and Day 2 Pupae (60hAPF). For pupal tissue, hindwing tissue was dissected using the wing vein landmarks shown, corresponding to the future adult position of the hindwing yellow bar (dissection scheme based on ***Hanly et al., 2019***). (**b**) Relative abundance of transcripts corresponding to the genes *cortex*, *domeless-truncated*, *domeless/washout* throughout developmental stages. (**c**) Log_2FoldChange for the genes *cortex*, *domeless-truncated (dome-t)*, *domeless/washout (dome-wash)* across developmental stages. Comparisons are for whole wing discs (Larvae, L) and across wing sections differing in the presence of a yellow bar in pupal wings (D1 and D2; see ***Figure 2—figure supplement 2***: for depiction of contrasts analysed). *Adjusted $p<0.05$; n/s = not significant. N = 3 for each bar plot.

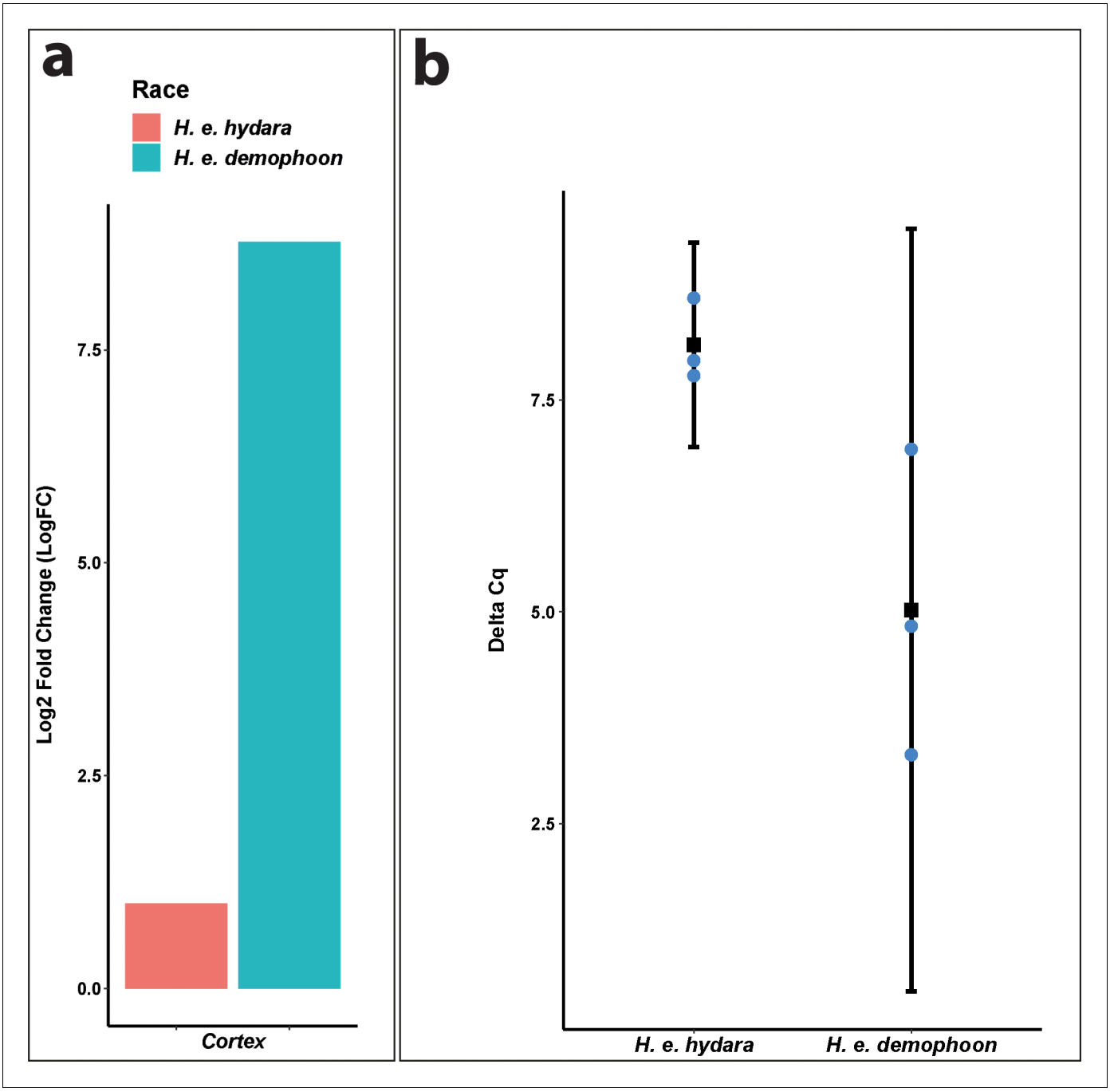

Figure 2—figure supplement 1. qPCR confirms direction of differential expression in Heliconius erato. (**a**) Cortex log2 fold change relative to *H. e. hydara* using delta CT. Data were normalised against the geometric average CT of three housekeeping genes *eF1a*, *rpL3*, and *polyABP*. (**b**) *Cortex* deltaCT in *H. e. hydara* and *H. e. demophoon*. Error bars represent the confidence interval for n = 3 (p=0.0444).

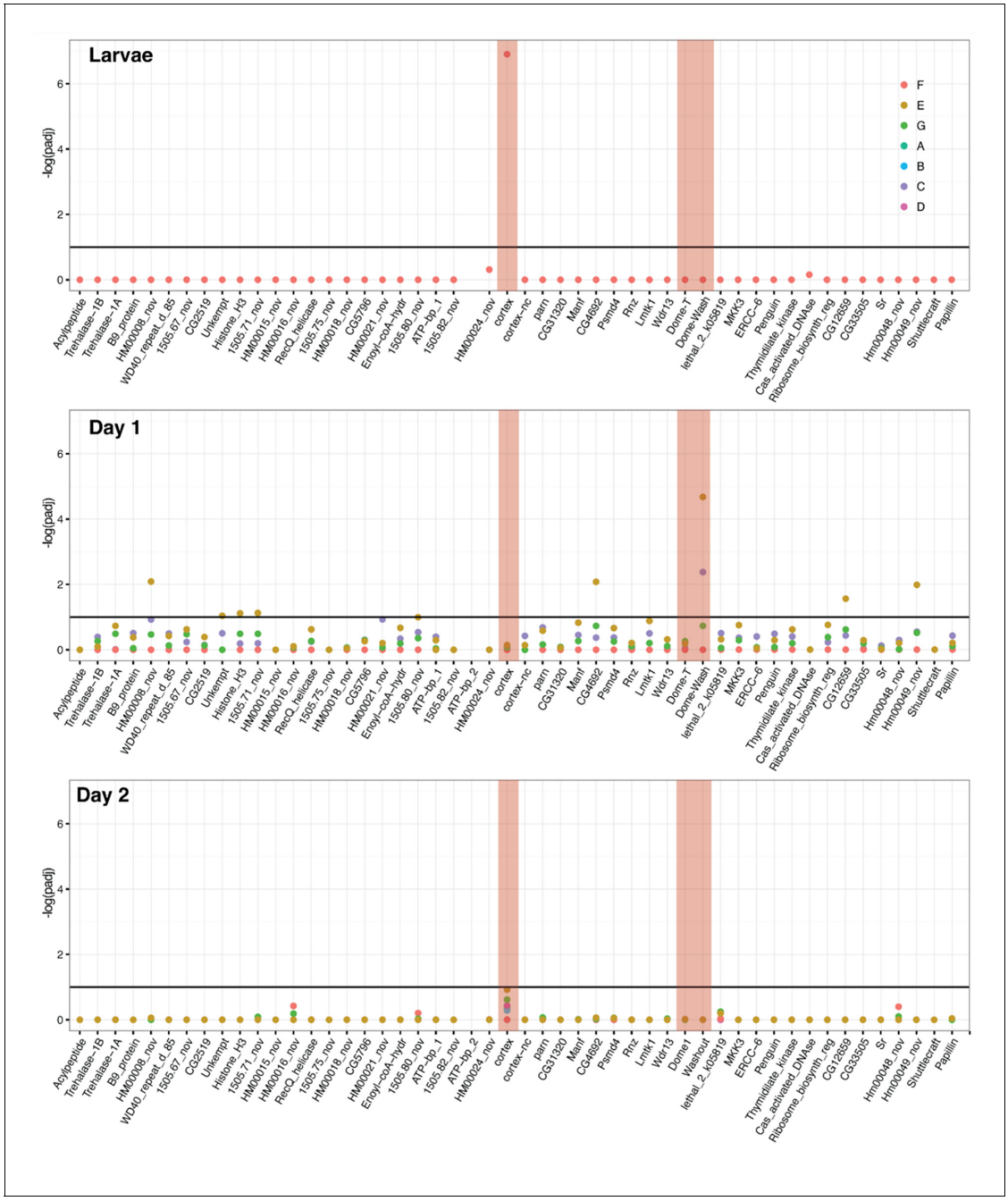

Figure 2—figure supplement 2. DGE analysis shows *cortex* and *dome/wash* are consistently differentially expressed between colour pattern races and pupal wing sections. Differential expression across the *cortex* locus in *H. erato*, shown as the negative log of the adjusted p-value (-log(padj)). Top: larvae, middle: Day 1 pupae, bottom, Day 2 pupae. See ***Figure 2—source data 4*** for gene IDs and homology with *H. melpomene*. The red shading highlights the genes *cortex*, *dome-T*, and *Dome-Wash*. The horizontal line indicates the cutoff for significance, at padj = 0.1. Colours are used for each of the contrasts, depicted in ***Figure 3***. In this analysis, genes were differentially expressed in contrast E and C (depictions of these contrasts are provided). E gives genes differentially regulated in black posterior compartment, and C gives genes differentially regulated in yellow anterior compartment.

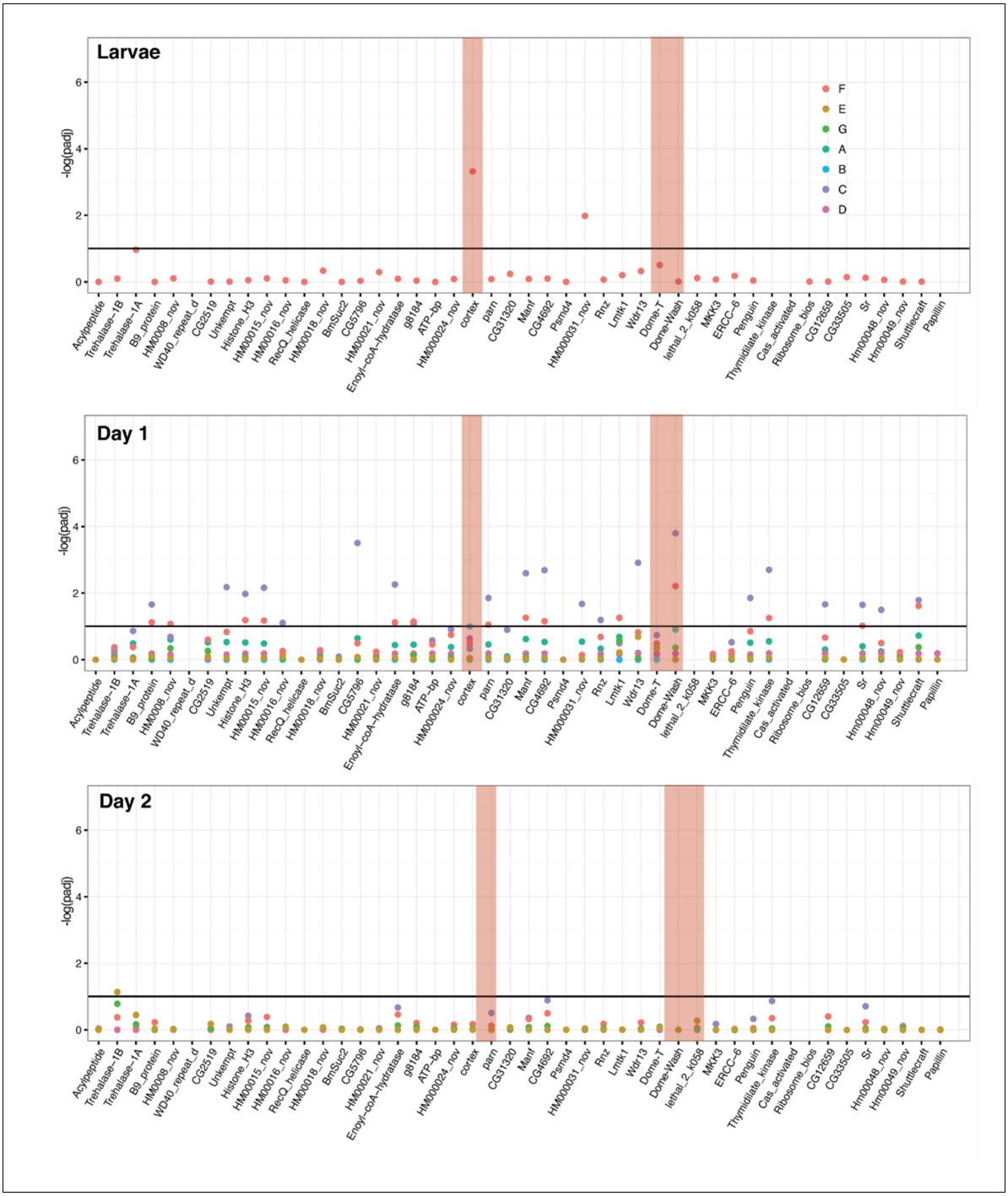

Figure 2—figure supplement 3. Differential expression across the *cortex* locus in *H. melpomene*, shown as the negative log of the adjusted p-value (–log(padj)). Top: larvae, middle: day one pupae, bottom, day two pupae. See ***Figure 2—source data 4*** for gene IDs and homology with *H. erato*. Red bars highlight the genes *cortex*, *Dome-T*, and *Dome-Wash*. The horizontal line indicates the cutoff for significance, at padj = 0.1. Colours are used for each of the contrasts, depicted in ***Figure 2—figure supplement 4***. In this analysis, genes were differentially expressed in contrast E, C, and F (depictions of these contrasts are provided). F is the difference between races, E gives genes differentially regulated in black posterior compartment, and C gives genes differentially regulated in yellow anterior compartment (these contrasts are depicted in cartoon form).

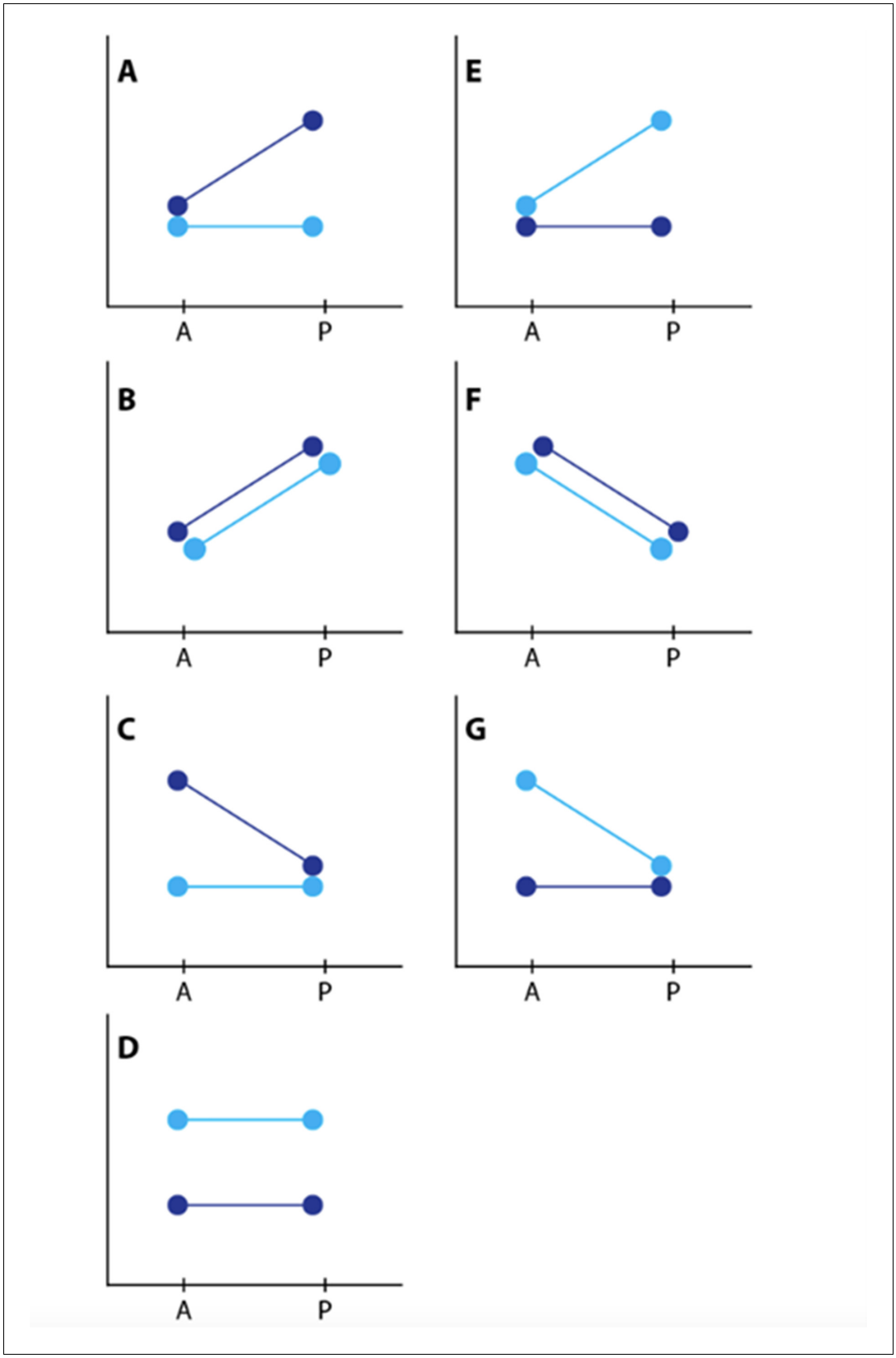

Figure 2—figure supplement 4. Depiction of contrasts. Dark blue represents the yellow races, *H. m. rosina* and *H. e. demophoon* from Panama. Light blue represents the black races, *H. m. melpomene* and *H. e. hydara* from Colombia.

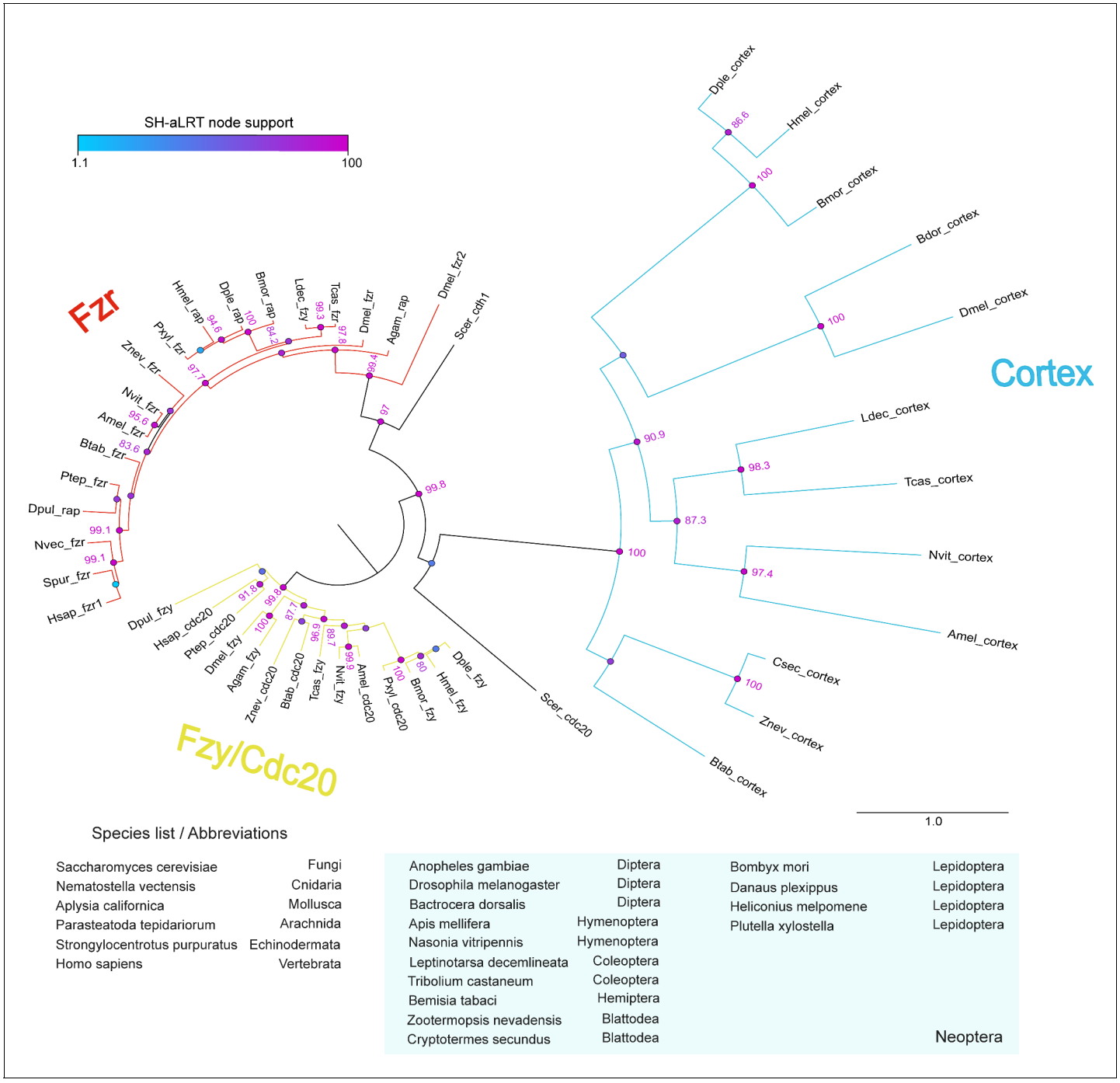

Species list / Abbreviations

Saccharomyces cerevisiae	Fungi
Nematostella vectensis	Cnidaria
Aplysia californica	Mollusca
Parasteatoda tepidariorum	Arachnida
Strongylocentrotus purpuratus	Echinodermata
Homo sapiens	Vertebrata

Anopheles gambiae	Diptera
Drosophila melanogaster	Diptera
Bactrocera dorsalis	Diptera
Apis mellifera	Hymenoptera
Nasonia vitripennis	Hymenoptera
Leptinotarsa decemlineata	Coleoptera
Tribolium castaneum	Coleoptera
Bemisia tabaci	Hemiptera
Zootermopsis nevadensis	Blattodea
Cryptotermes secundus	Blattodea

Bombyx mori	Lepidoptera
Danaus plexippus	Lepidoptera
Heliconius melpomene	Lepidoptera
Plutella xylostella	Lepidoptera

Neoptera

Figure 2—figure supplement 5. analysis of the cdc20/cdh1 family reveals Cortex is a derived and insect-specific derivative of cdc20. Full-length protein homologs retrieved from TBLASTN searches were used to generate a curated alignment with MAFFT/Guidance2 with a column threshold of 0.5. TBLASTN searches against arthropod genome and transcriptome NCBI repositories did not recover Cortex homologues outside of the Neoptera lineage. The maximum-likelihood tree was constructed with W-IQ-TREE with the 'Auto' function to find a best-fit model of substitution. Colour circles indicate the scores of SH-like approximate likelihood ratio tests (SH-aLRT) computed over 1000 replicates, with numeric values for scores > 80. Scale bar indicates amino-acid substitutions per site. Abbreviations: fzy, fizzy; fzr, fizzy-related; rap, retina aberrant pattern (syn. fzr).

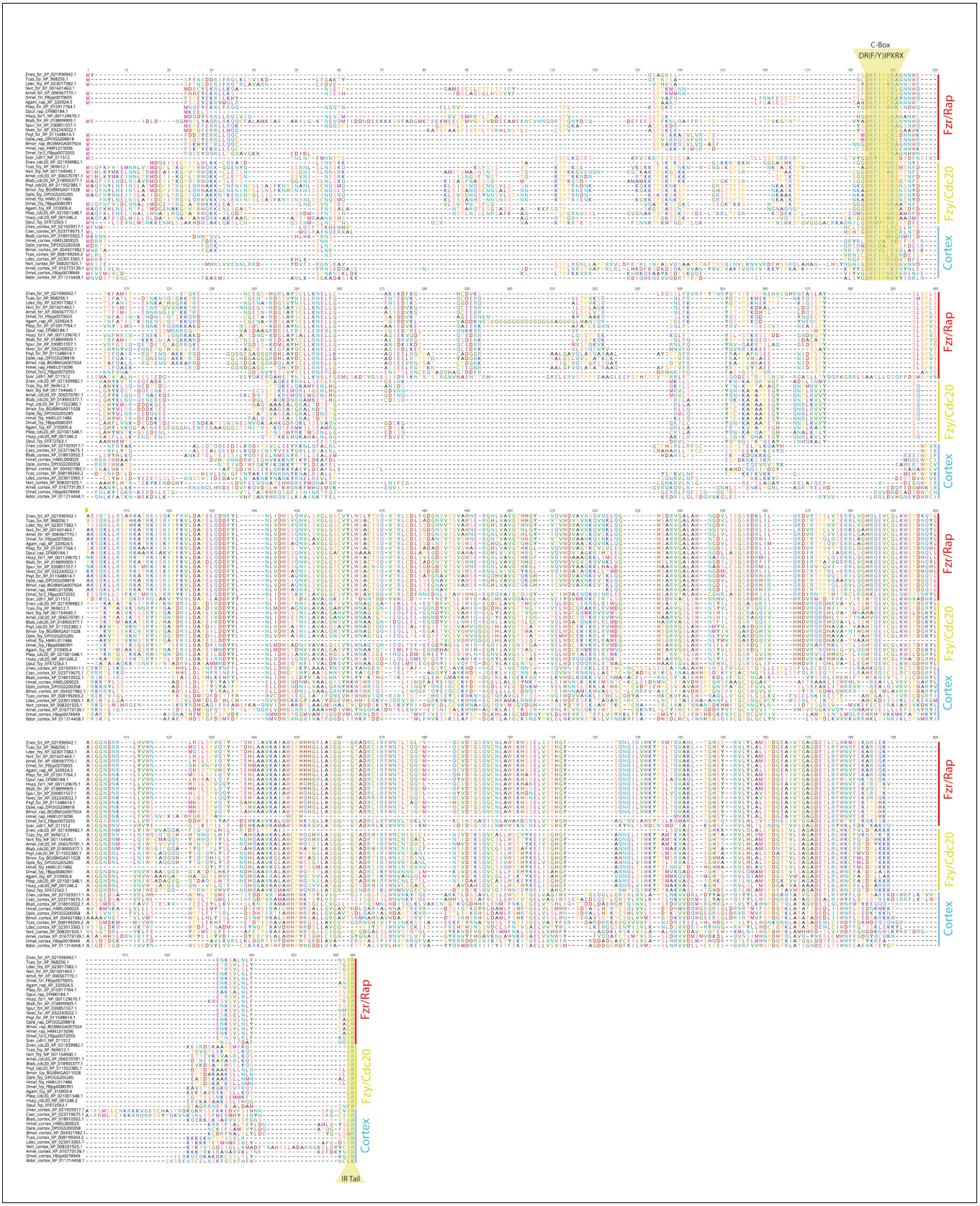

Figure 2—figure supplement 6. Full Cdc20 family protein alignments (see legend in ***Figure 2—figure supplement 5*** for abbreviations). The conserved C-box motif, necessary for interaction with the APC/C and the IR are highlighted.

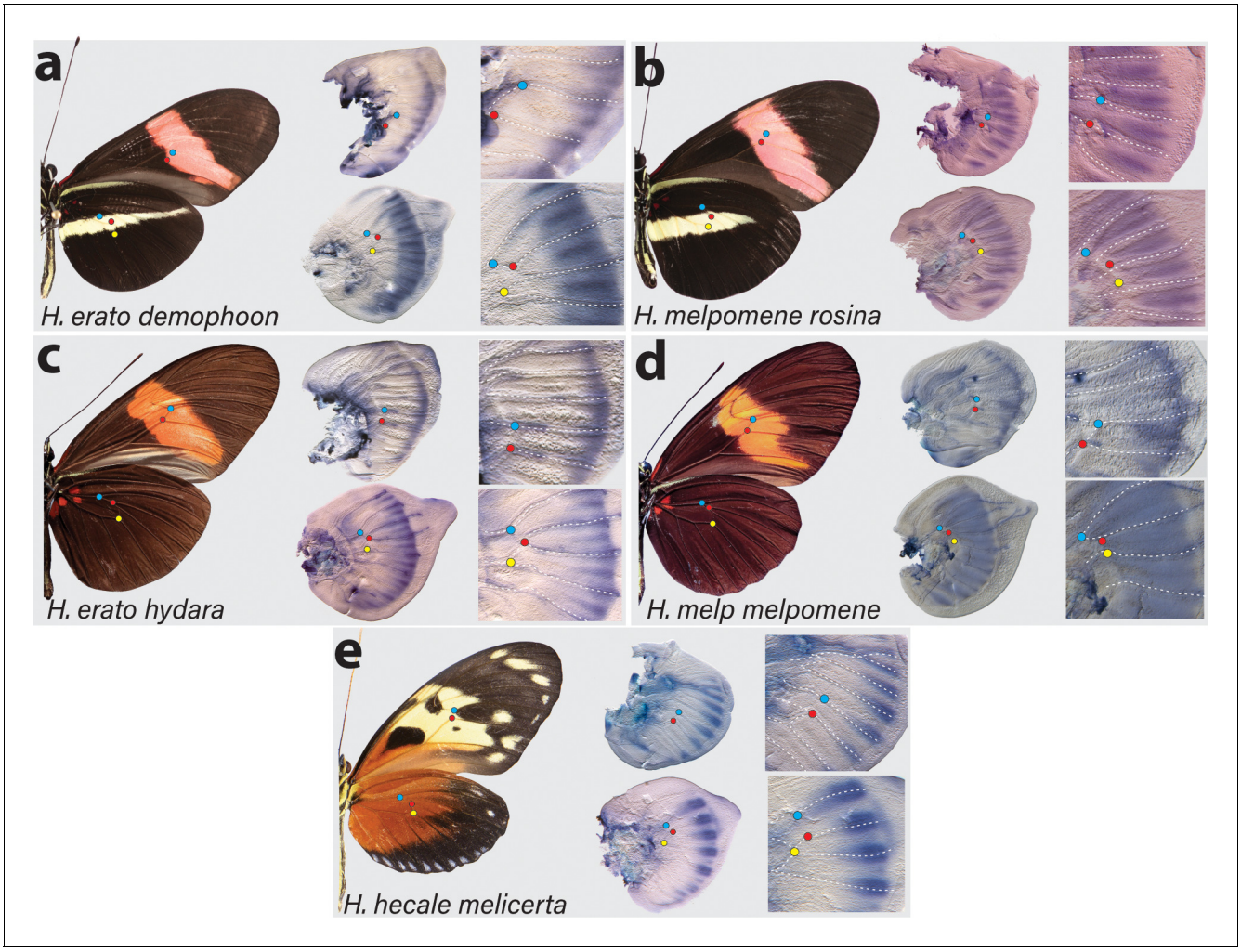

Figure 3. Expression of *cortex* transcripts in *Heliconius melpomene*, *Heliconius erato*, and *Heliconius hecale* fifth-instar wing discs. *Cortex* expression in fifth-instar wing discs is restricted to the distal end of both forewings and hindwings in all species and morphs analysed. In *H. erato*, expression is strongest at the intervein midline but extends across vein compartments in *H. erato demophoon* (**a**), whereas it is more strongly localised to the intervein midline in *H. erato hydara* (**c**). In *H. melpomene rosina* (**b**), *cortex* localises in a similar manner to *H. erato demophoon*, with stronger expression again observed at the intervein midline, whereas expression in *H. melpomene melpomene* (**d**) extends more proximally. Expression in *H. hecale melicerta* (**e**) is strongest at the distal wing vein margins. Coloured dots represent homologous vein landmarks across the wings.

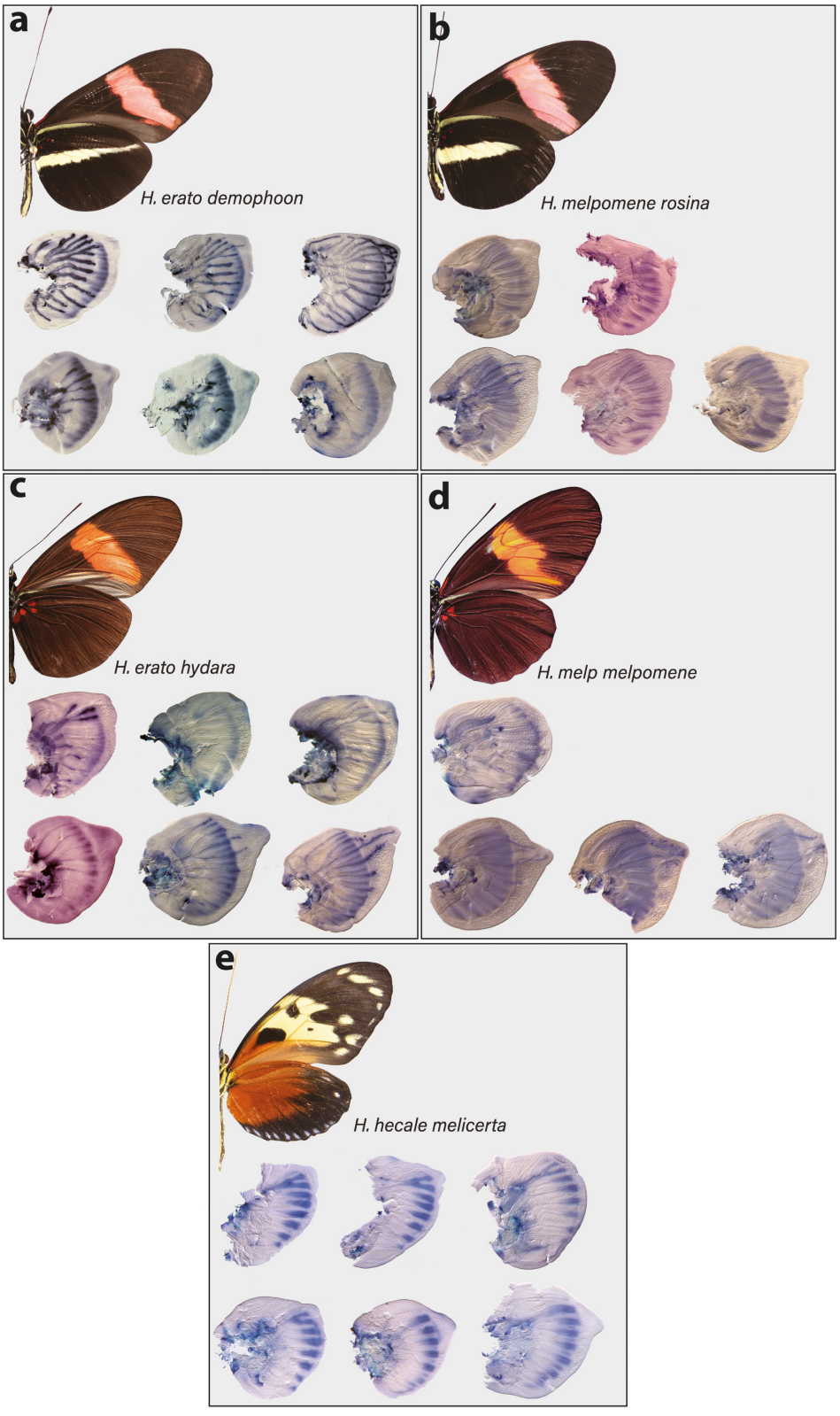
a
H. erato demophoon
b
H. melpomene rosina
c
H. erato hydara
d
H. melp melpomene
e
H. hecale melicerta

Figure 3—figure supplement 1. Distal expression of *cortex* in *Heliconius* fifth-instar imaginal discs. In *H. erato*, *cortex* expression is strongest at the distal end of the wing throughout fifth-instar development, with stronger intervein expression in *H. erato hydara*. In *H. melpomene*, *cortex* expression extends further proximally, with expression seen throughout the wing in *H. melpomene melpomene*.

Figure 4. *Cortex* loss-of-function transforms scale identity across the entire wing surface of *Heliconius erato*. Phenotypes of *cortex* mKO across *H. erato* morphs reveal a loss of melanic (Type II) and red (Type III) scales and transformation to Type I (yellow or white) scales. Affected regions are not spatially restricted and span both distal and proximal portions of forewings and hindwings. The scale transformation extends to all scale types, including the wing border scales (red arrow head in (**a**)), and across the red band elements, where mutant scales transform to white, as well as some showing an intermediate phenotype (blue arrow heads in (**b**)). A positional effect is observed in some morphs, where ectopic Type I scales are either white or yellow depending on their position along the wing (*H. erato cyrbia*, (**c**)). Ectopic Type I scales can be induced from both melanic and red scales, switching to either white or yellow depending on wing position and morph. Boundaries between Wild-type (WT) to mutant scales are highlighted (dotted white line).

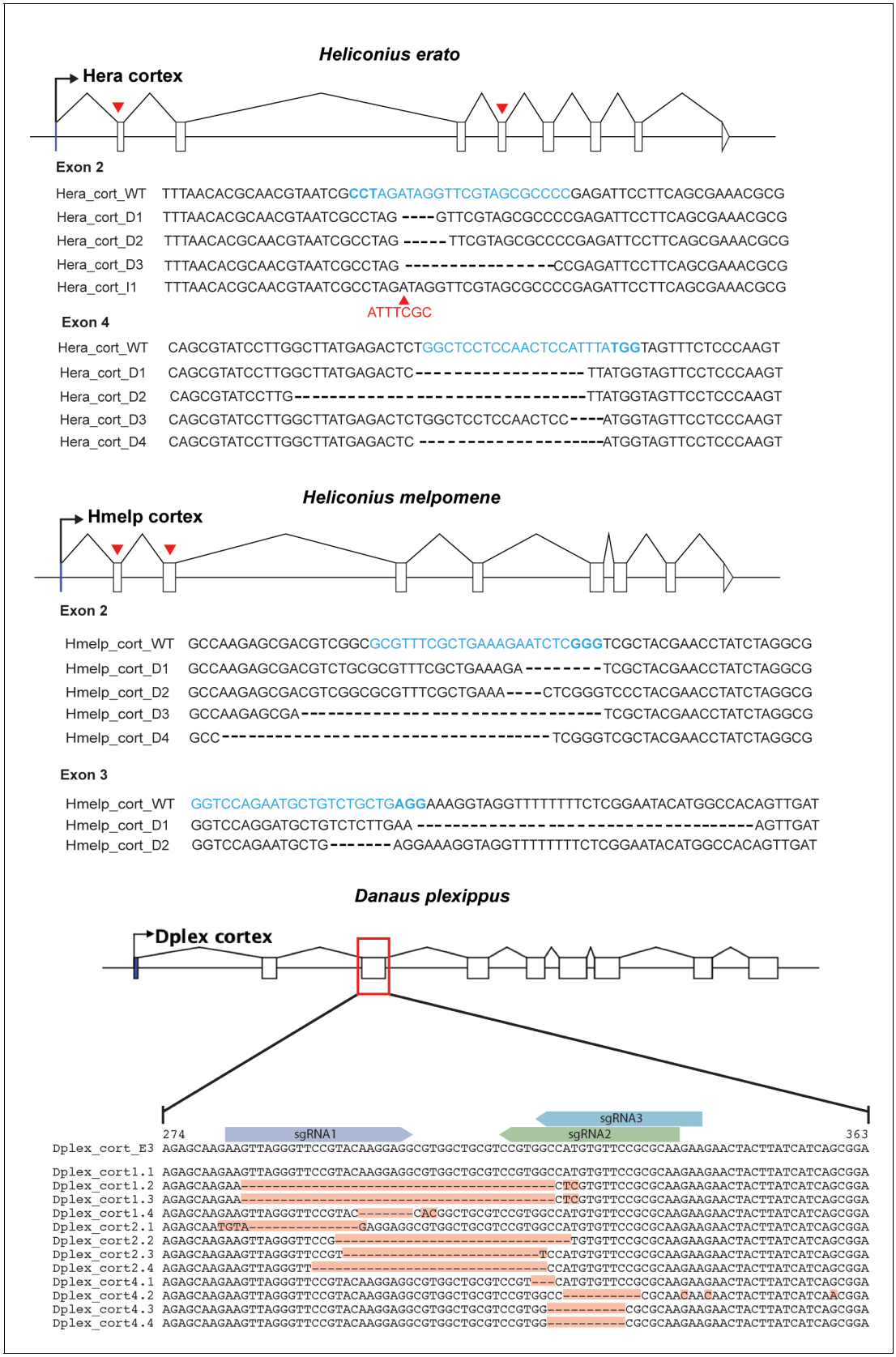

Figure 4—figure supplement 1. CRISPR mutagenesis confirmed through sanger sequencing. Gene models for cortex are shown for both *H. erato*, *H. melpomene* and *D. plexippus*. Red arrows indicate positions of sgRNAs that were genotyped in CRISPR experiments. Recovered sequences showing

Figure 4—figure supplement 1 continued on next page

Figure 4—figure supplement 1 continued

evidence of editing as a result of CRISPR mutagenesis are shown. Target sequences are shown in blue and PAM site highlighted in bold. For *H. erato* exon 2, we recovered a sequence containing a 7 bp insertion (indicated with red arrowhead, I2).

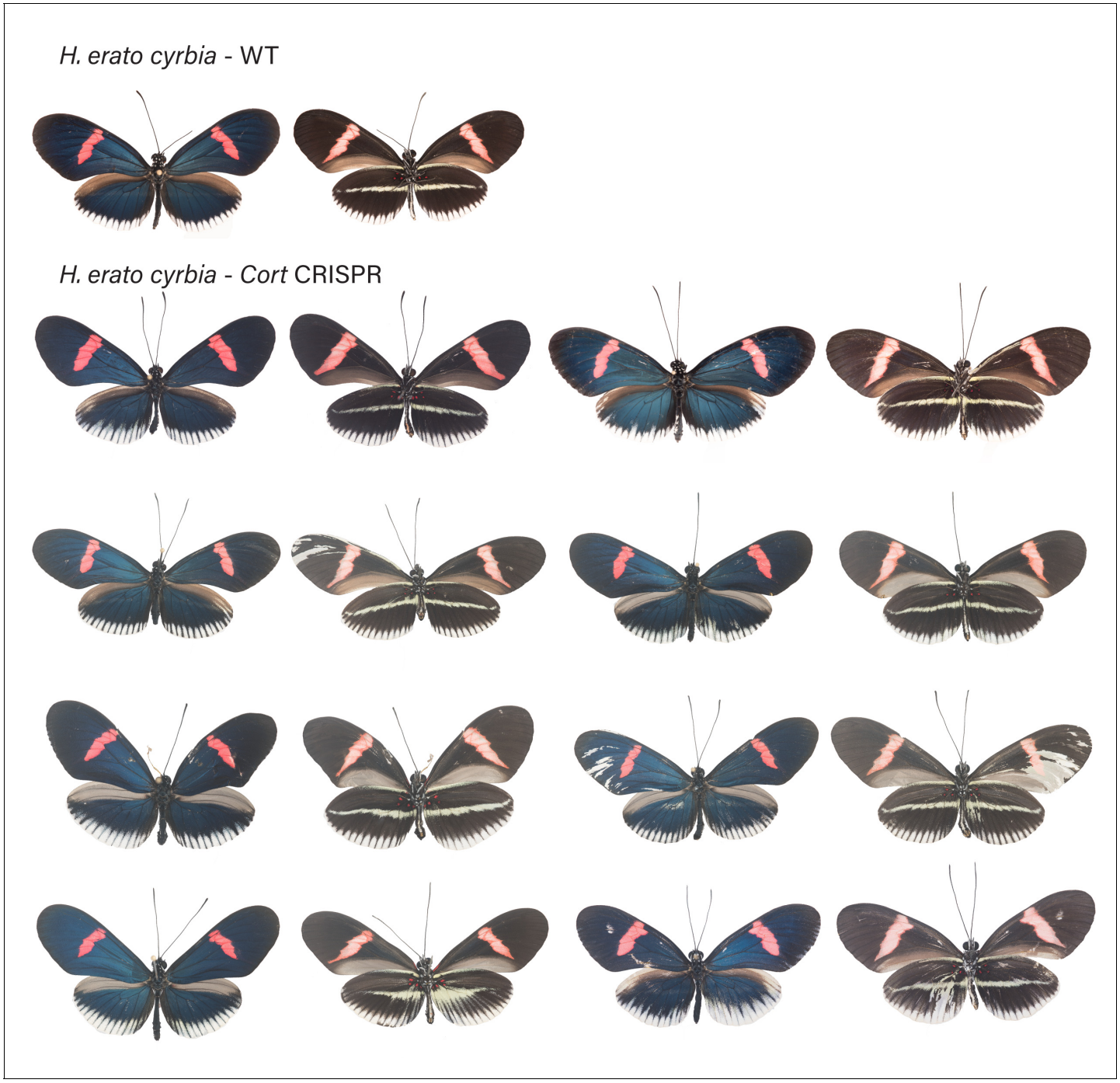

Figure 4—figure supplement 2. *H. erato cyrbia* wild-type (WT), alongside *cortex* mKO individuals recovered in CRISPR experiments. Dorsal and ventral sides shown for each mutant.

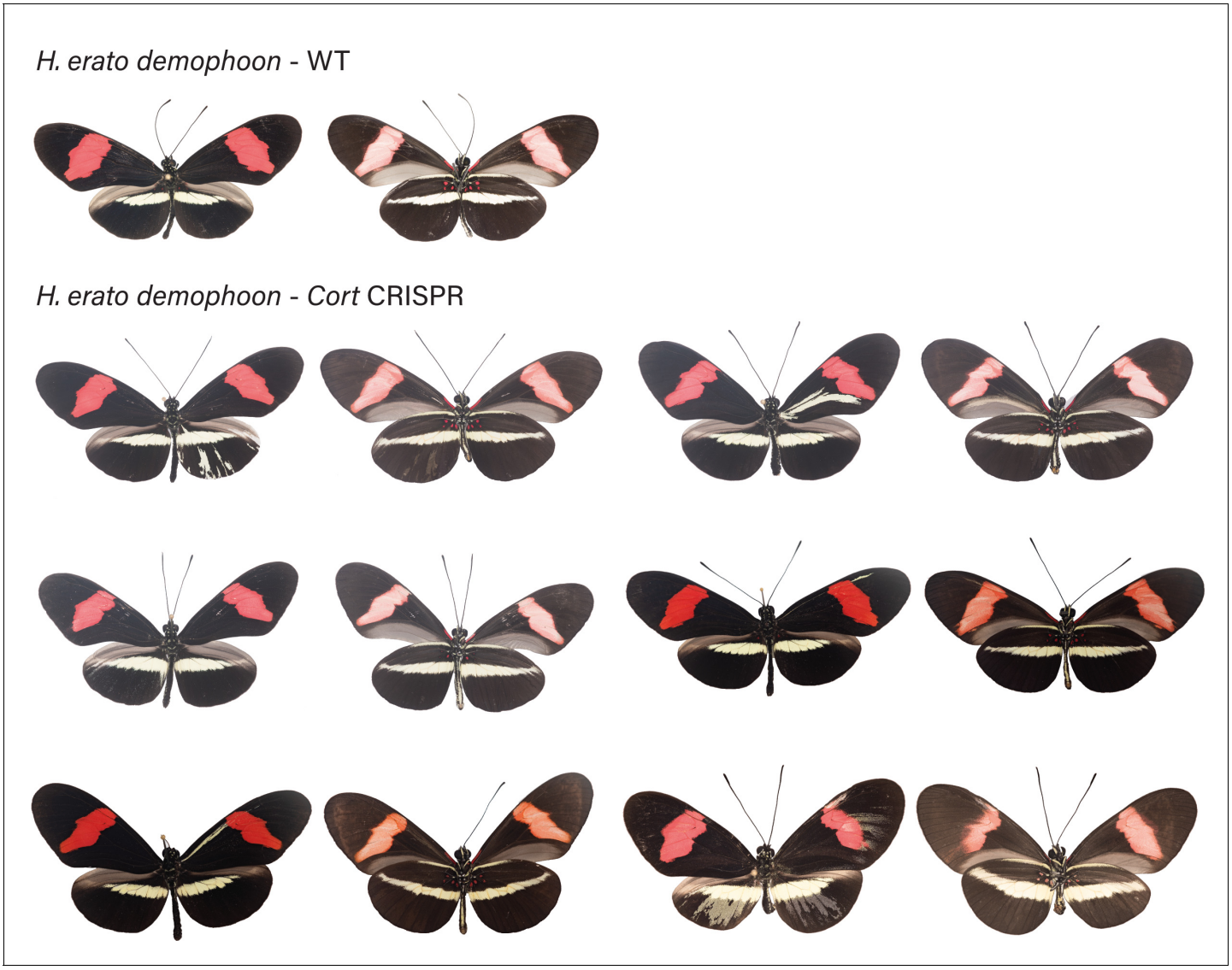

Figure 4—figure supplement 3. *H. erato demophoon* wild-type (WT), alongside *cortex* mKO individuals recovered in CRISPR experiments. Dorsal and ventral sides shown for each mutant.

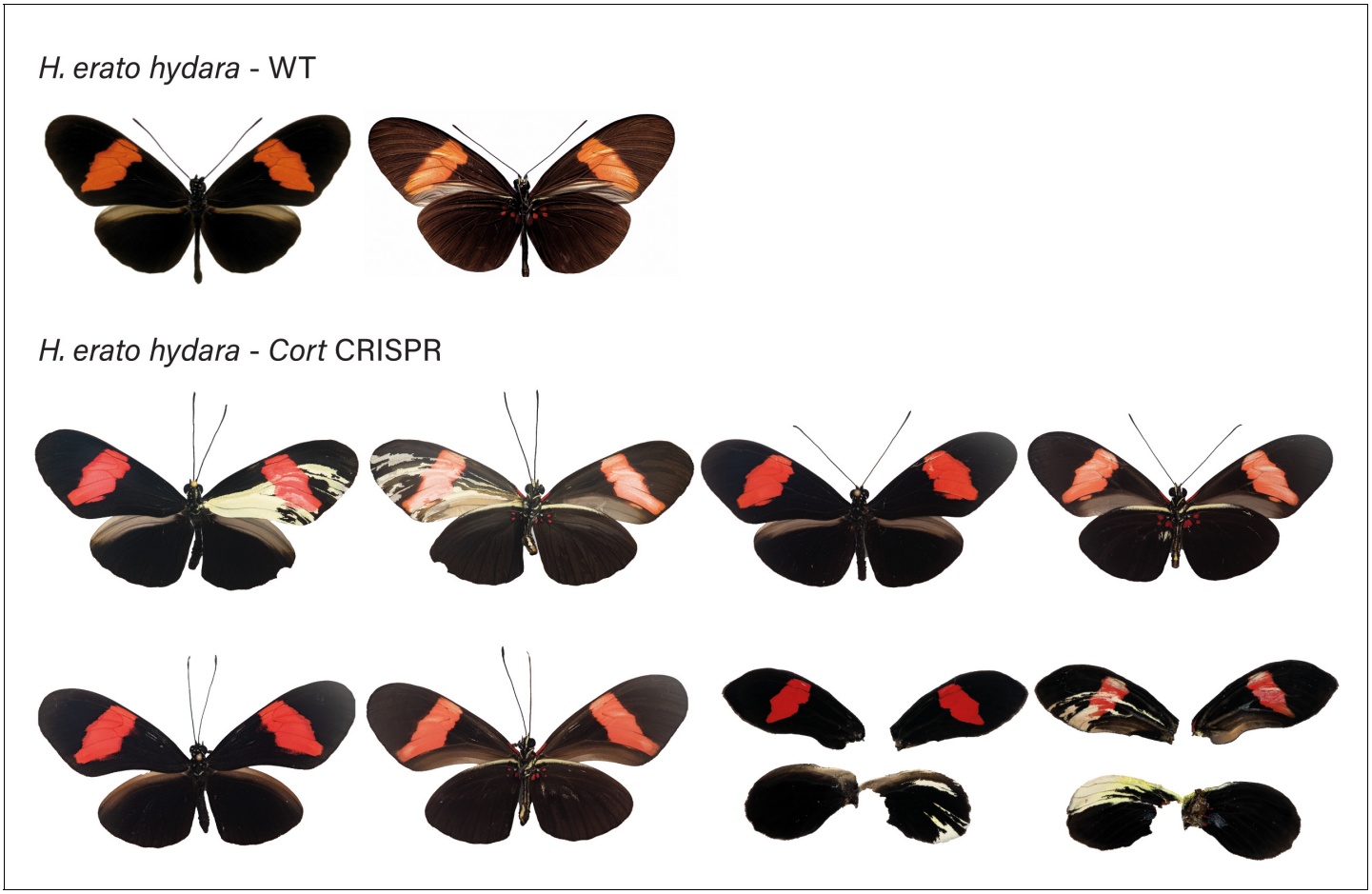

Figure 4—figure supplement 4. *H. erato hydara* wild-type (WT), alongside *cortex* mKO individuals recovered in CRISPR experiments. Dorsal and ventral sides shown for each mutant.

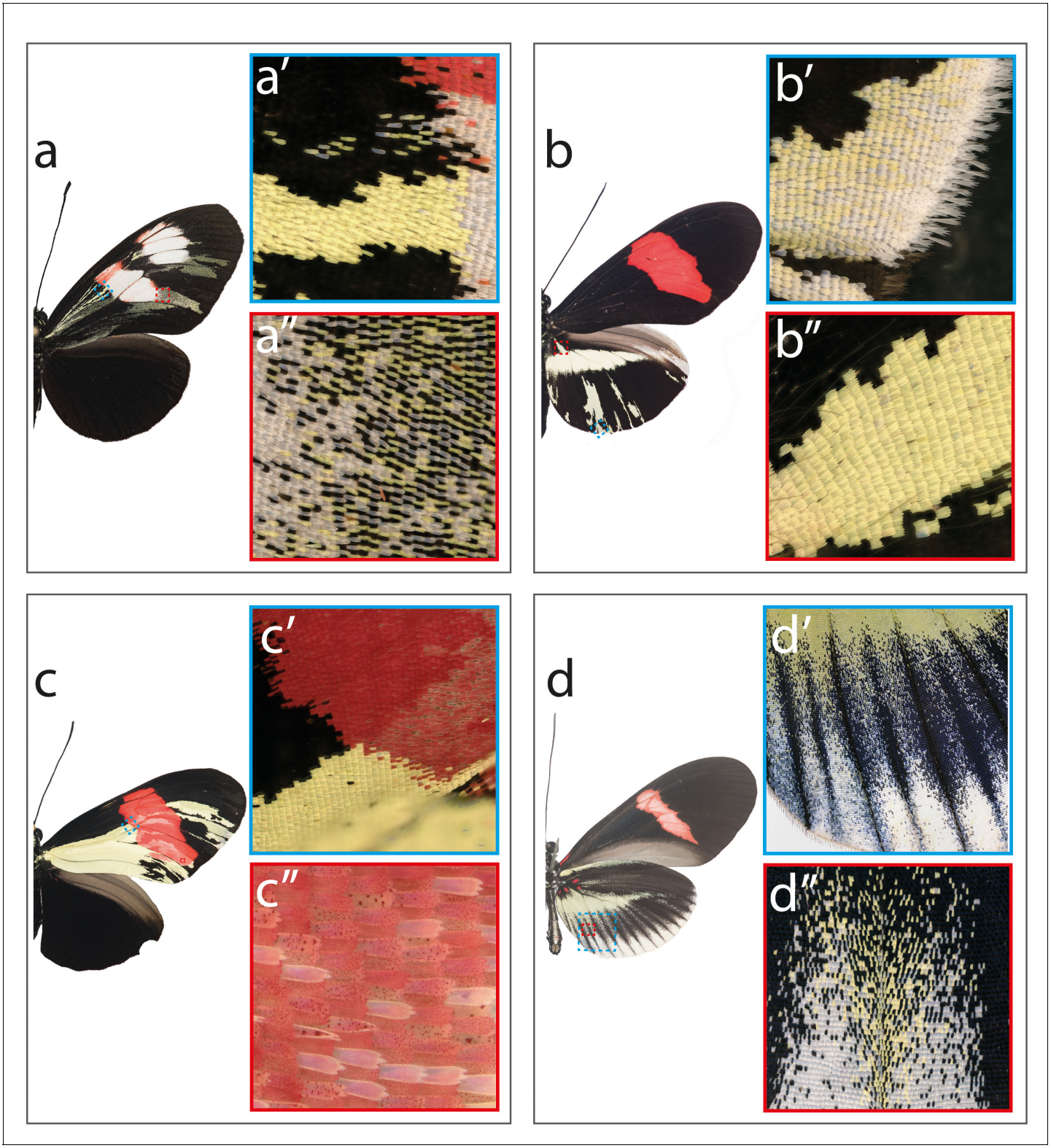

Figure 4—figure supplement 5. Mutant close-ups illustrating variety of effects caused by *cortex* mKO. (**a**) *H. melpomene plesseni* showing mutant clones across proximal forewing (**a′**) as we as more distal areas, where cover scales are more affected (**a′′**). (**b**) *H. erato demophoon* showing cortex mKO effects on elongated border scales (**b′**), and scale located anterior to yellow bar element (**b′′**). (**c**) *H. erato hydara* showing clones extending into forewing red band (**c′**) and asymmetric deposition of red pigment across the affected red band region (**c′′**). (**d**) *H. erato cyrbia* illustrates positional effect of *cortex* mKO where posterior hindwing scales shift to white, while anterior scales shift to yellow (**d′**and **d′′**).

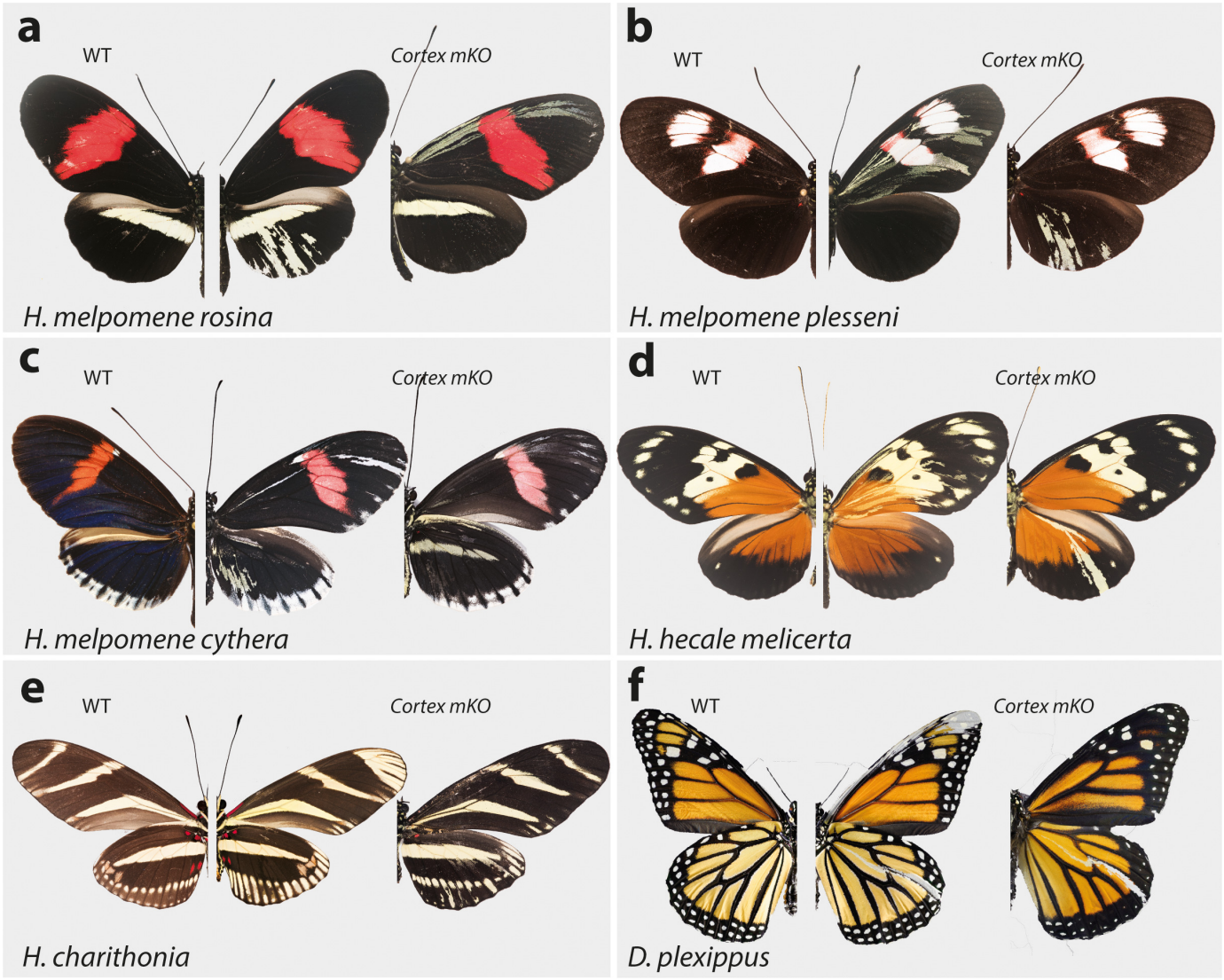

Figure 5. *Cortex* function is conserved across *Heliconius* and Nymphalids Phenotypes of *cortex* mKO across *H. melpomene* colour pattern morphs. (**a–c**) reveal *cortex* has a conserved function in switching scale cell fates, as in *H. erato*. This function is also conserved in outgroups to *H. melpomene* and *H. erato* (*H. hecale melicerta* and *H. charithonia* respectively (**d–e**)) as well as in distantly diverged nymphalids (*D. plexippus* (**f**)). Left; wild-type, middle and right; *cortex* mKO.

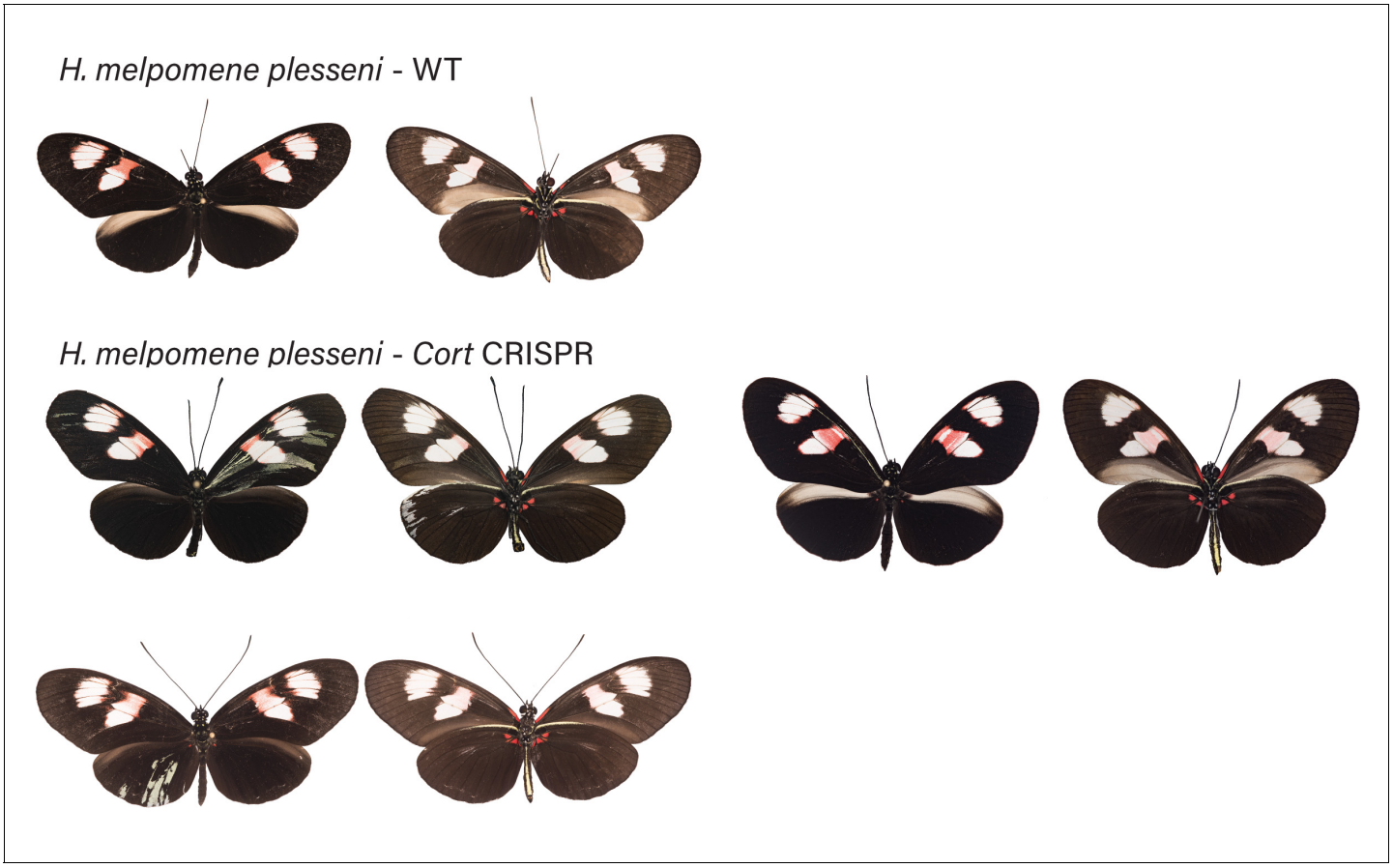

Figure 5—figure supplement 1. *H. melpomene plesseni* wild-type (WT), alongside *cortex* mKO individuals recovered in CRISPR experiments. Dorsal and ventral sides shown for each mutant.

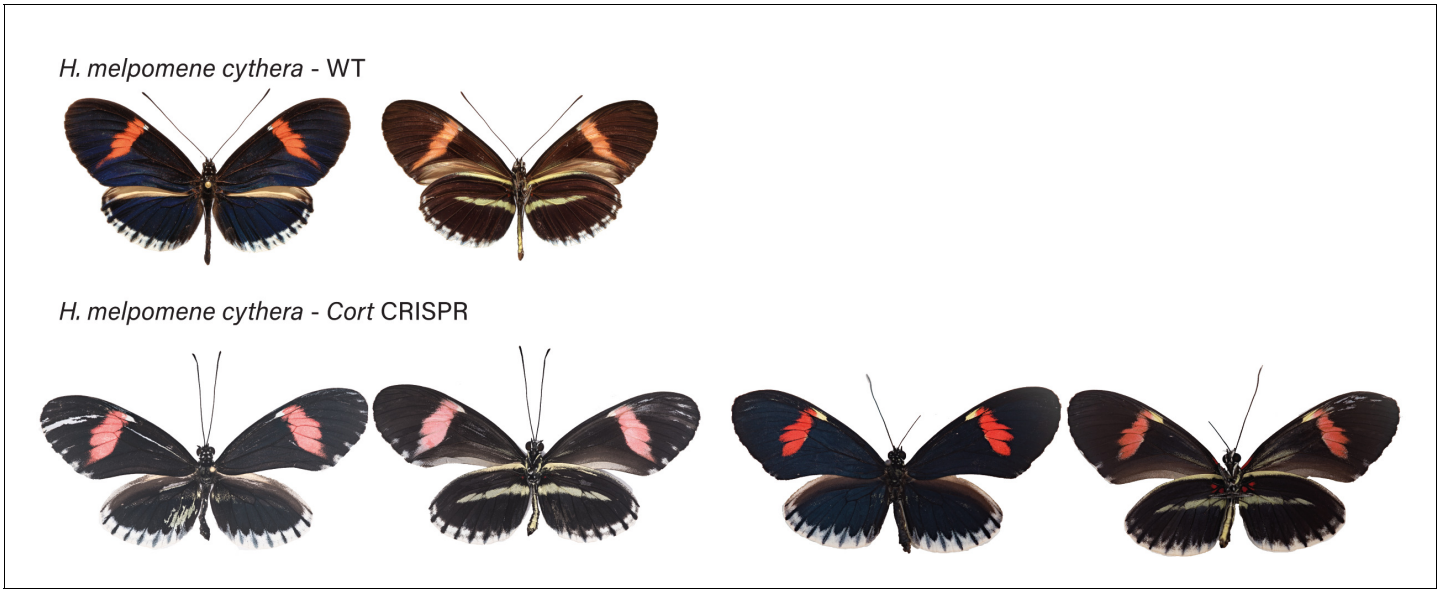

Figure 5—figure supplement 2. *H. melpomene cythera* wild-type (WT), alongside *cortex* mKO individuals recovered in CRISPR experiments. Dorsal and ventral sides shown for each mutant.

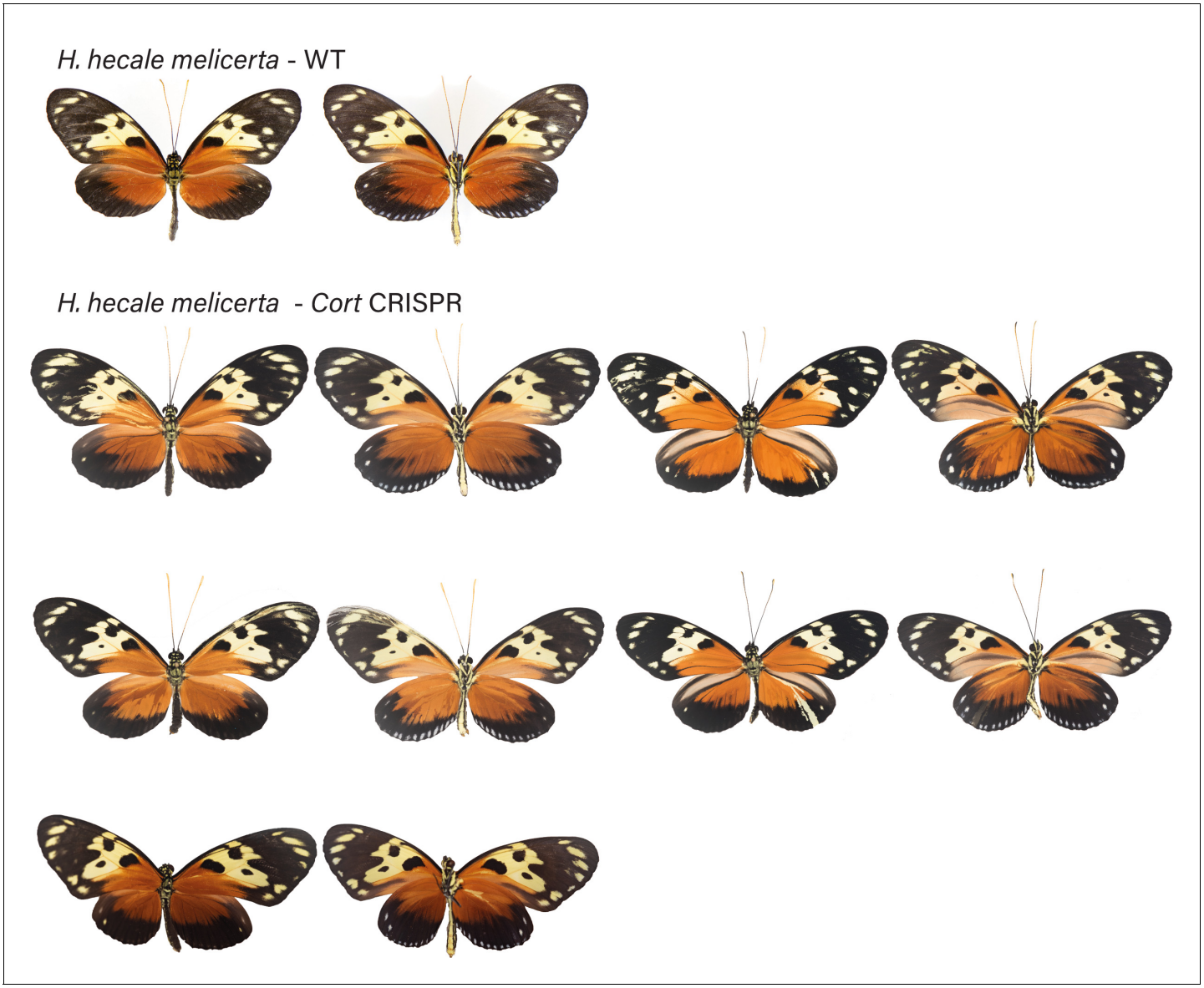

Figure 5—figure supplement 3. *H. hecale melicerta* wild-type (WT), alongside *cortex* mKO individuals recovered in CRISPR experiments. Dorsal and ventral sides shown for each mutant.

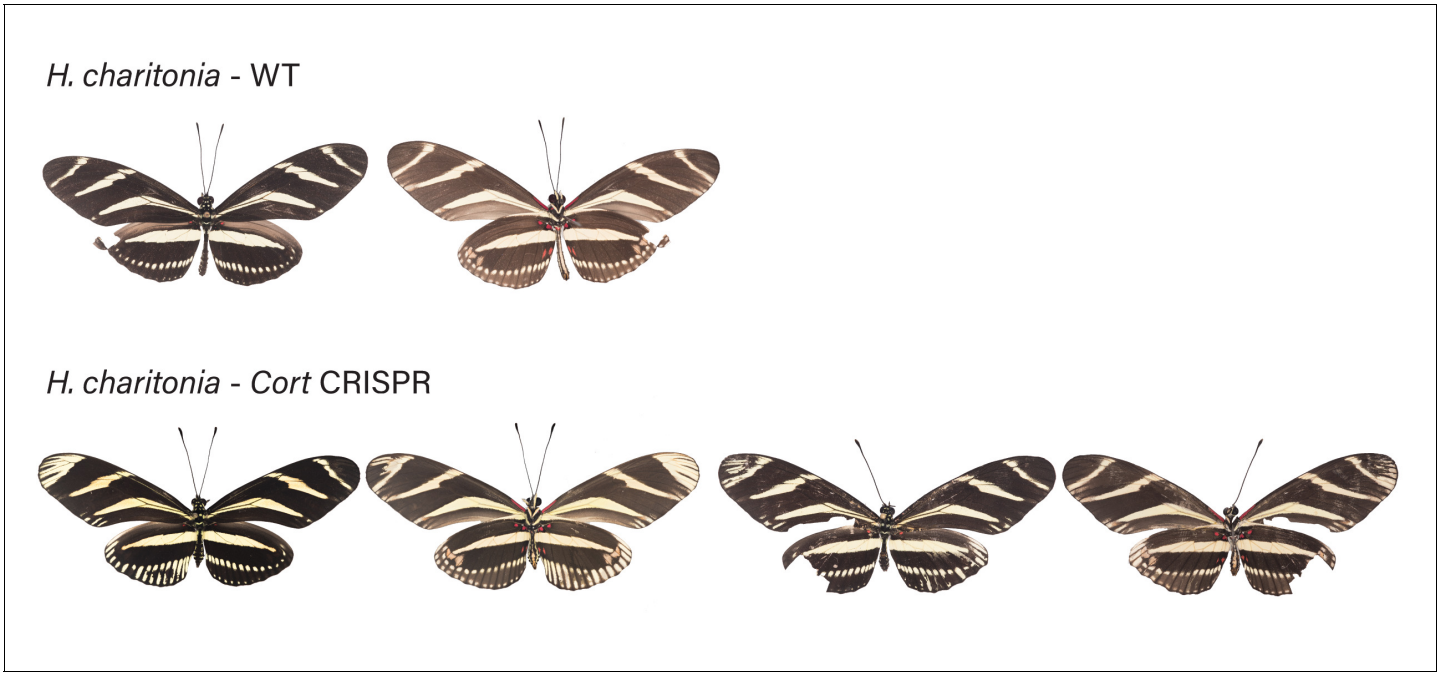

Figure 5—figure supplement 4. *H. charithonia* wild-type (WT), alongside *cortex* mKO individuals recovered in CRISPR experiments. Dorsal and ventral sides shown for each mutant.

Figure 5—figure supplement 5. *Danaus plexippus* wild-type (WT), alongside *cortex* CRE mKO individuals recovered in CRISPR experiments. Dorsal and ventral sides shown for each mutant.

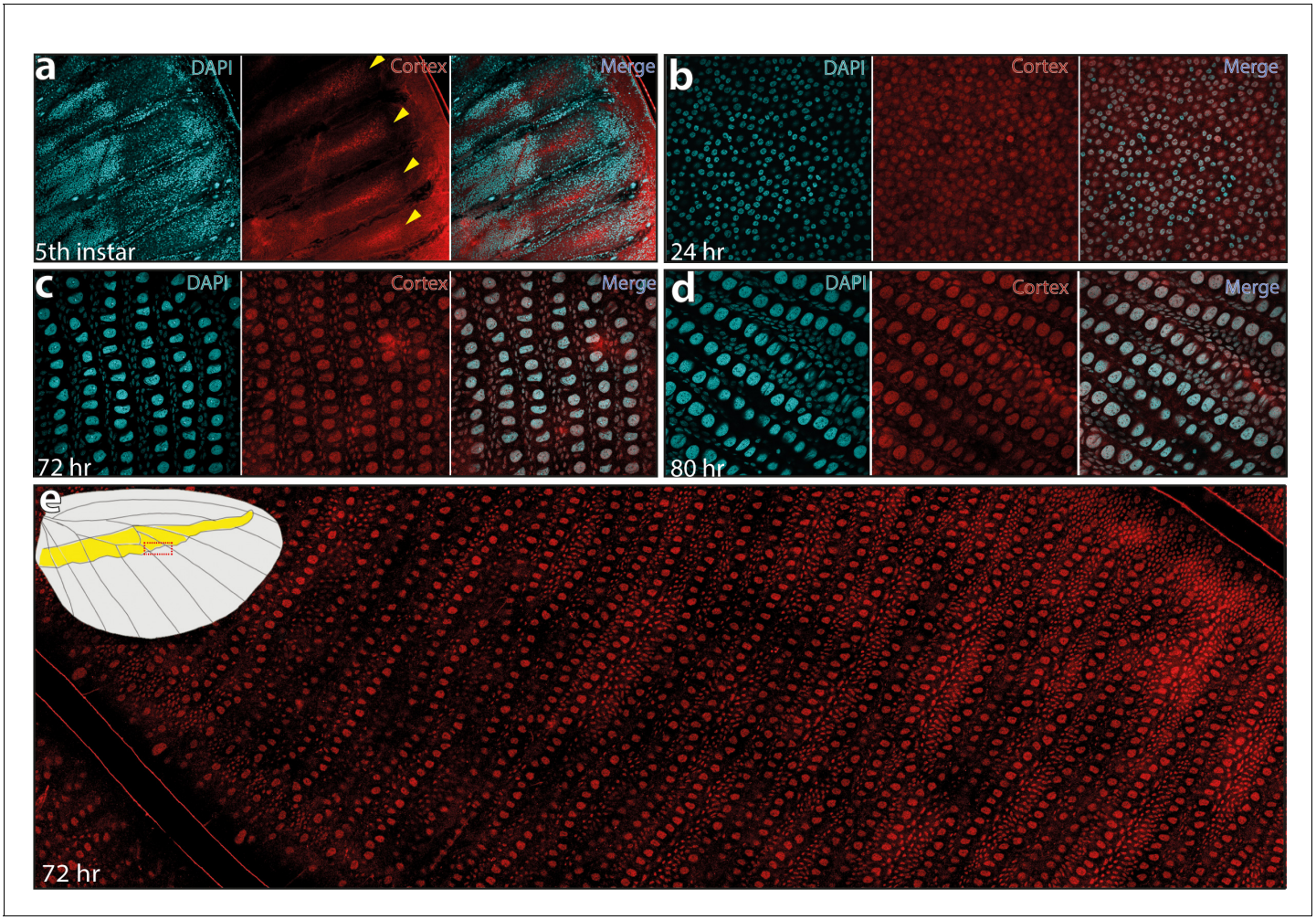

Figure 6. Cortex protein localises across the wings in *H. erato demophoon*. Antibody stainings reveal Cortex protein is localised at the distal intervein midline in fifth-instar wing discs (yellow arrowheads) (**a**). At 24 hr APF, the protein is detected across the wing and localised strongly to the cell nuclei (**b**). This localisation continues at 72 hr APF(**c**) and 80 APF (**d**). In each panel, leftmost insert shows nuclei stained with DAPI (magenta), middle insert with Cortex antibody detected with a secondary alexa-fluor 555 conjugated antibody (red), and right insert shows both channels merged into a composite image. No appreciable difference in localisation is detected across presumptive pattern elements at 72 hr APF (**e**). The magnified portion of the imaged wing is indicated in the wing cartoon in the top left corner of (**e**).

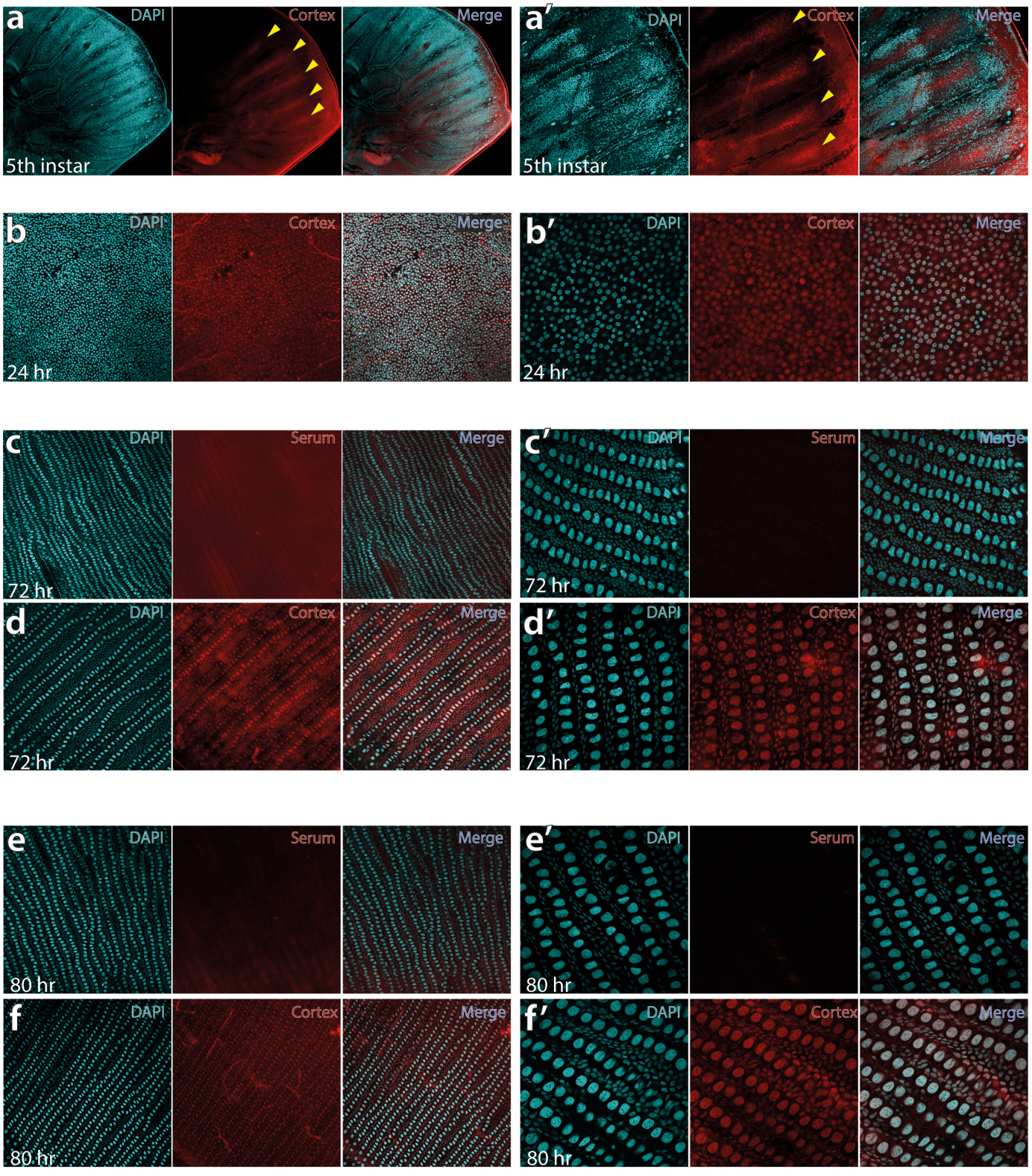

Figure 6—figure supplement 1. Fifth-instar larval wing disc showing intervein localisation of Cortex protein at 10× (**a**) and 30× magnification of the same area (**a′**). Pupal wings sampled at 24 hr post-pupation at 20× magnification (**b**) and 60× magnification (**b′**) show nuclear localisation of Cortex

Figure 6—figure supplement 1 continued on next page

Figure 6—figure supplement 1 continued

protein. At this stage, the hexagonal organisation of future scale cells is apparent, with the middle cell eventually differentiating into the scale cell. Pupal wings were stained with a negative control using the pre-immune serum at 72 hr, shown at 20× (**c**) and 60× (**c'**), reveal no evidence of nuclear signal. Using the same confocal settings with Cortex antibody at 72 hr reveals nuclear localisation at 30x magnification (**d**) and 60× magnification (**d'**). The nuclear staining is also absent in control serum samples at 80 hr post-pupation (**e and e'**), with nuclear localisation persisting in Cortex antibody incubated samples at 80 hr post-pupation (**f and f'**).

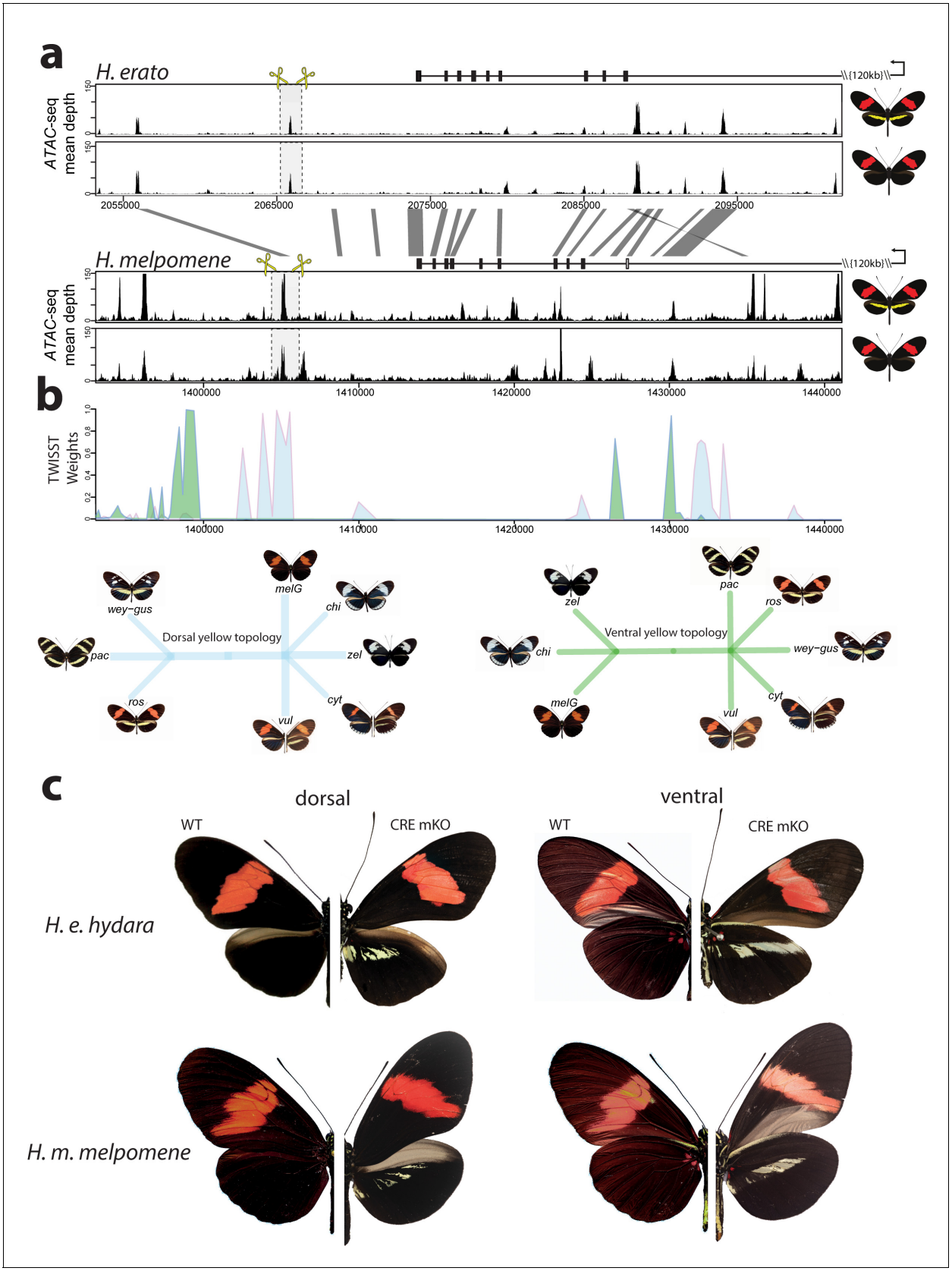

Figure 7. Modular CREs control the presence of the yellow band in *Heliconius melpomene* and *Heliconius erato*. (a) Chromatin accessibility as measured by mean sequence depth for *ATAC-seq* traces in *H. erato* (top) and *H. melpomene* (bottom) in fifth-instar caterpillar hindwings in yellow

Figure 7 continued on next page

Figure 7 continued

banded and black morphs. The gene model for *cortex* is shown above the traces (black rectangles are coding exons, white rectangle non-coding exon, lines are introns, direction of transcription is indicated by an arrow). The transcription start site is around 120 kb from the first coding exon of *cortex*. Positions of sgRNAs used for peak excision are shown (yellow scissors). Regions with >75% sequence identity between *H. melpomene* and *H. erato* are indicated by grey lines. (**b**) Twisst analysis results showing high genetic association for the presence of a yellow bar in *H. melpomene* populations with a ventral (ventral topology) or dorsal (dorsal topology) yellow bar. Abbreviations for twisst morphs: wey-gus = *H. cydno weymeri-gustavi*, chi = *H. cydno chioneus*, zel = *H. cydno zelinde*, pac = *H. pachinus*, ros = *H. melpomene rosina*, melG = *H. melpomene melpomene* French Guiana, vul = *H. melpomene vulcanus*, cyt = *H. melpomene cythera*. (**c**) *Cortex* loss-of-function at the yellow bar CREs affect scales only in the presumptive yellow bar region. CRE KO affects both dorsal (left) and ventral (right) hindwings.

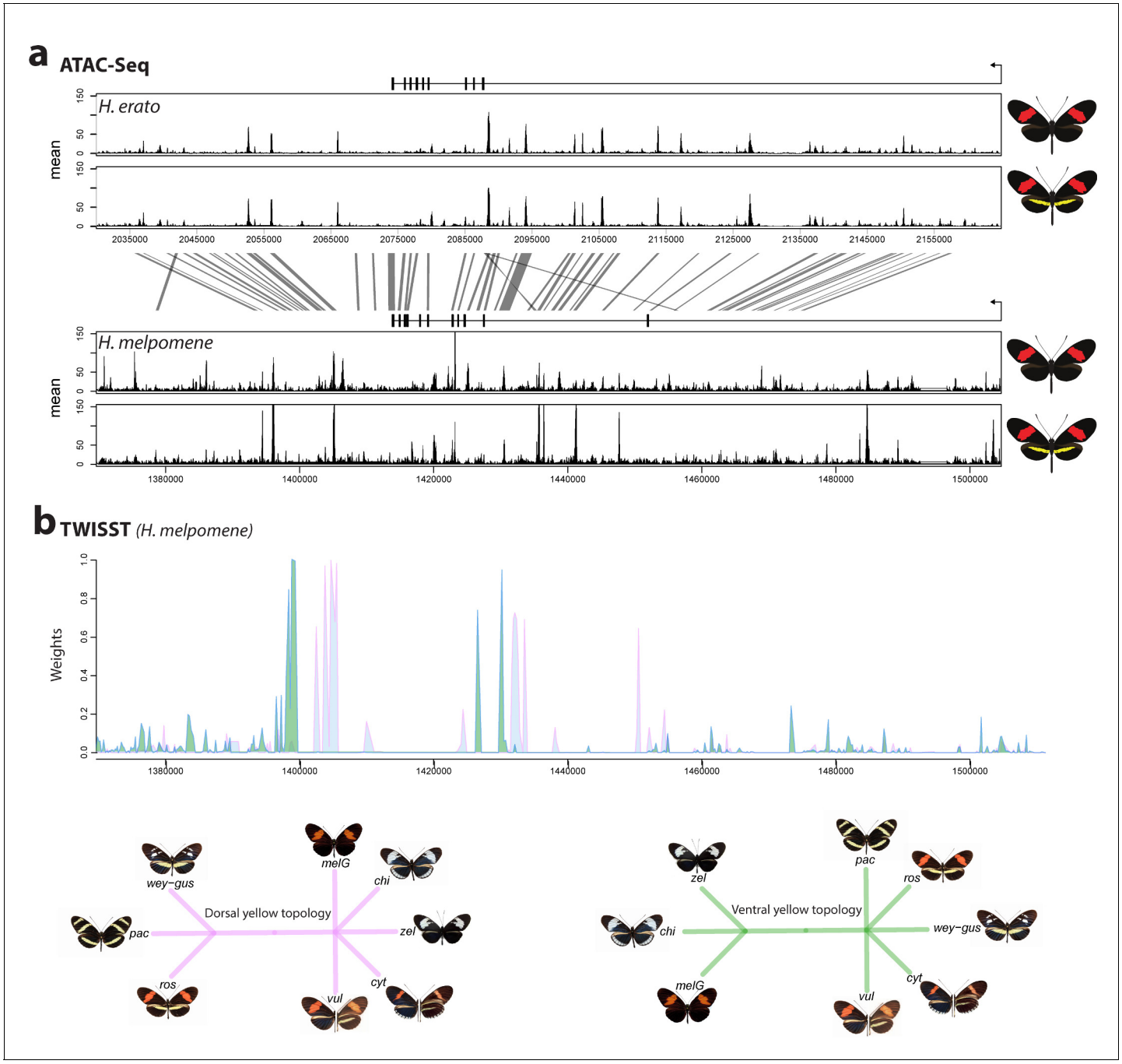

Figure 7—figure supplement 1. The *cortex* locus is characterised by many accessible chromatin peaks as revealed by *ATAC-seq*. Mean sequence depth for *ATAC-Seq* traces in *H.erato* (top) and *H. melpomene* (bottom) in fifth-instar caterpillar hindwings in yellow banded and black morphs. The gene model for *cortex* is shown above the traces (black rectangles are coding exons, lines are introns, direction of transcription is indicated by an arrow). 95% sequence identity between *H. melpomene* and *H.erato* is indicated by grey lines. (**b**) Twisst analysis results showing high support for the presence of a yellow bar in *H.melpomene* populations with a ventral (ventral topology) or dorsal (dorsal topology) yellow bar. Tree topologies used to calculate weightings are shown. Abbreviations for twisst morphs: wey-gus = *H. cydno weymeri-gustavi*, chi = *H. cydno chioneus*, zel = *H. cydno zelinde*, pac = *H. pachinus*, ros = *H. melpomene rosina*, vul = *H. melpomene vulcanus*, cyt = *H. melpomene cythera*, melG = *H. melpomene melpomene* (French Guiana).

Figure 7—figure supplement 2. *H. melpomene melpomene* wild-type (WT), alongside *cortex* CRE mKO individuals recovered in CRISPR experiments. Dorsal and ventral sides shown for each mutant.

Figure 7—figure supplement 3. *H. erato hydara* wild-type (WT), alongside *cortex* CRE mKO individuals recovered in CRISPR experiments. Dorsal and ventral sides shown for each mutant.

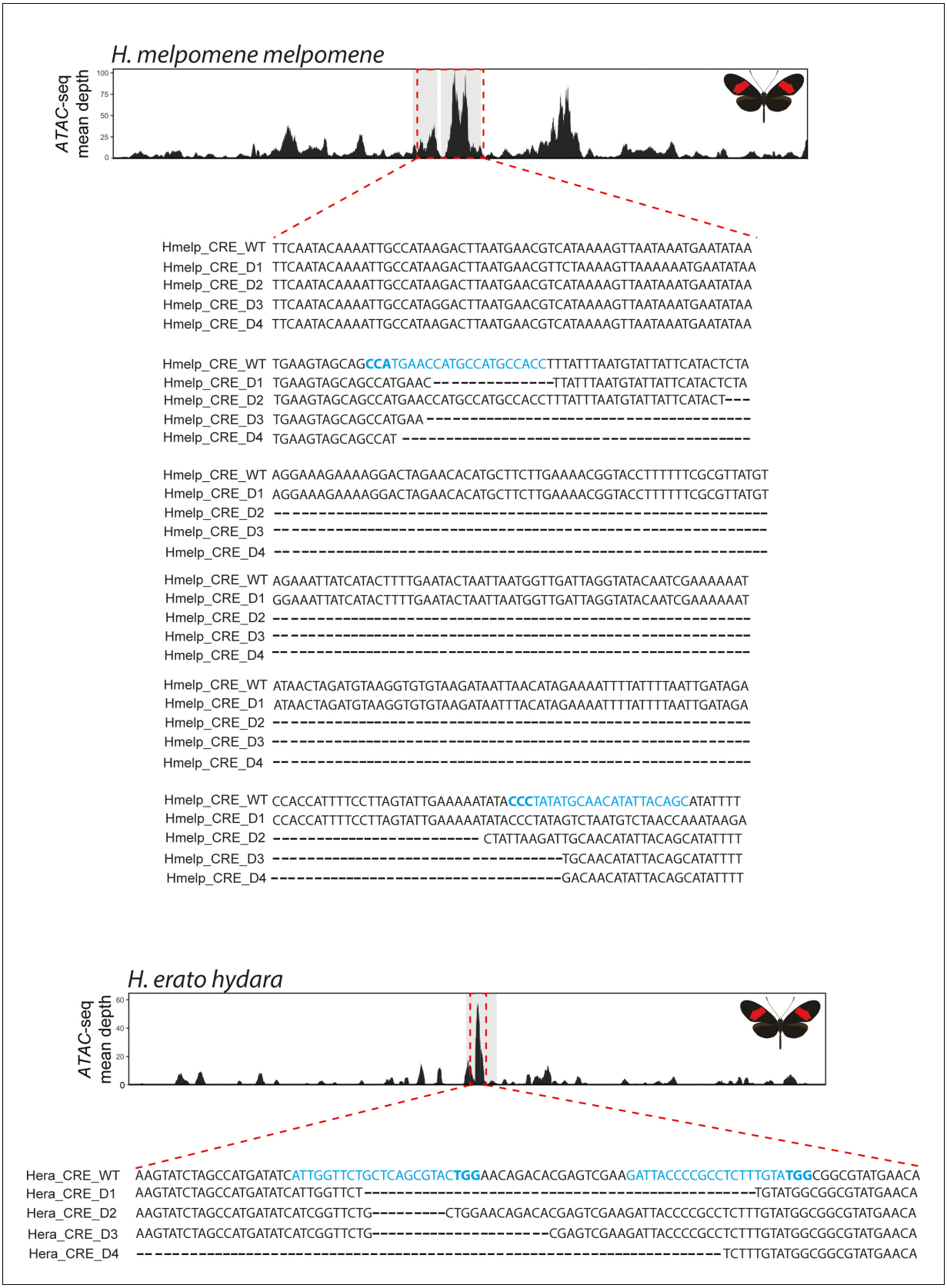
H. melpomene melpomene
ATAC-seq mean depth
100
75
50
25
0
Hmelp_CRE_WT TTCAATACAAAATTGCCATAAGACTTAATGAACGTCATAAAAGTTAATAAATGAATATAA
Hmelp_CRE_D1 TTCAATACAAAATTGCCATAAGACTTAATGAACGTTCTAAAAGTTAAAAAATGAATATAA
Hmelp_CRE_D2 TTCAATACAAAATTGCCATAAGACTTAATGAACGTCATAAAAGTTAATAAATGAATATAA
Hmelp_CRE_D3 TTCAATACAAAATTGCCATAGGACTTAATGAACGTCATAAAAGTTAATAAATGAATATAA
Hmelp_CRE_D4 TTCAATACAAAATTGCCATAAGACTTAATGAACGTCATAAAAGTTAATAAATGAATATAA
Hmelp_CRE_WT TGAAGTAGCAGCCATGAACCATGCCATGCCACCTTTATTTAATGTATTATTCATACTCTA
Hmelp_CRE_D1 TGAAGTAGCAGCCATGAAC----------TTATTTAATGTATTATTCATACTCTA
Hmelp_CRE_D2 TGAAGTAGCAGCCATGAACCATGCCATGCCACCTTTATTTAATGTATTATTCATACT---
Hmelp_CRE_D3 TGAAGTAGCAGCCATGAA----------
Hmelp_CRE_D4 TGAAGTAGCAGCCAT----------
Hmelp_CRE_WT AGGAAAGAAAAGGACTAGAACACATGCTTCTTGAAAACGGTACCTTTTTTCGCGTTATGT
Hmelp_CRE_D1 AGGAAAGAAAAGGACTAGAACACATGCTTCTTGAAAACGGTACCTTTTTTCGCGTTATGT
Hmelp_CRE_D2 ----------
Hmelp_CRE_D3 ----------
Hmelp_CRE_D4 ----------
Hmelp_CRE_WT AGAAATTATCATACTTTTGAATACTAATTAATGGTTGATTAGGTATACAATCGAAAAAAT
Hmelp_CRE_D1 GGAAATTATCATACTTTTGAATACTAATTAATGGTTGATTAGGTATACAATCGAAAAAAT
Hmelp_CRE_D2 ----------
Hmelp_CRE_D3 ----------
Hmelp_CRE_D4 ----------
Hmelp_CRE_WT ATAACTAGATGTAAGGTGTGTAAGATAATTAACATAGAAAATTTTATTTTAATTGATAGA
Hmelp_CRE_D1 ATAACTAGATGTAAGGTGTGTAAGATAATTTACATAGAAAATTTTATTTTAATTGATAGA
Hmelp_CRE_D2 ----------
Hmelp_CRE_D3 ----------
Hmelp_CRE_D4 ----------
Hmelp_CRE_WT CCACCATTTTCCTTAGTATTGAAAAATATACCCTATATGCAACATATTACAGCATATTTT
Hmelp_CRE_D1 CCACCATTTTCCTTAGTATTGAAAAATATACCCTATAGTCTAATGTCTAACCAAATAAGA
Hmelp_CRE_D2 ---------- CTATTAAGATTGCAACATATTACAGCATATTTT
Hmelp_CRE_D3 ----------TGCAACATATTACAGCATATTTT
Hmelp_CRE_D4 ----------GACAACATATTACAGCATATTTT
H. erato hydara
ATAC-seq mean depth
60
40
20
0
Hera_CRE_WT AAGTATCTAGCCATGATATCATTGGTTCTGCTCAGCGTACTGGAACAGACACGAGTCGAAGATTACCCCGCCTCTTTGTATGGCGGCGTATGAACA
Hera_CRE_D1 AAGTATCTAGCCATGATATCATTGGTTCT----------TGTATGGCGGCGTATGAACA
Hera_CRE_D2 AAGTATCTAGCCATGATATCATCGGTTCTG---------CTGGAACAGACACGAGTCGAAGATTACCCCGCCTCTTTGTATGGCGGCGTATGAACA
Hera_CRE_D3 AAGTATCTAGCCATGATATCATCGGTTCTG----------CGAGTCGAAGATTACCCCGCCTCTTTGTATGGCGGCGTATGAACA
Hera_CRE_D4 ----------TCTTTGTATGGCGGCGTATGAACA

Figure 7—figure supplement 4. Genotyping at the *H. melpomene* and *H. erato* CRE confirms CRISPR-induced deletions. Targeted ATAC-seq peak shown above (red dotted rectangle), as well as alignment between wild-type and recovered deletions. Guides highlighted in blue with PAM sequence in bold.

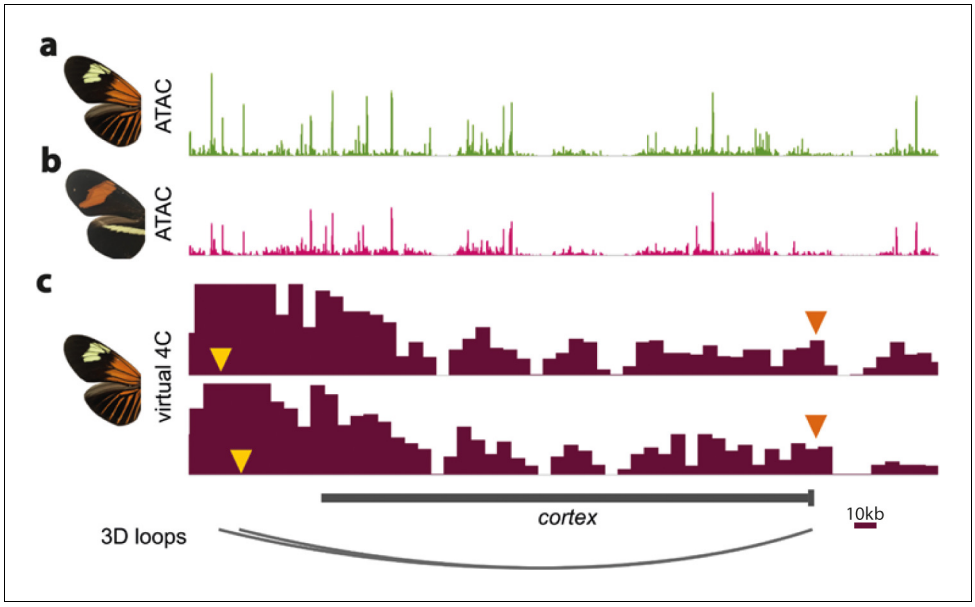

Figure 7—figure supplement 5. ATAC-Seq traces at the *cortex* locus for day three old pupal wings in *H. erato lativitta* (**a**) and *H. erato demophoon* (**b**). Virtual 4C plots showing significant interactions ($p<0.05$) for the CREs assayed in the CRISPR experiments (yellow arrowheads) with the *cortex* promoter (orange arrowheads) (**c**). Data from ***Lewis et al., 2019***. Scale bar = 10 kb.

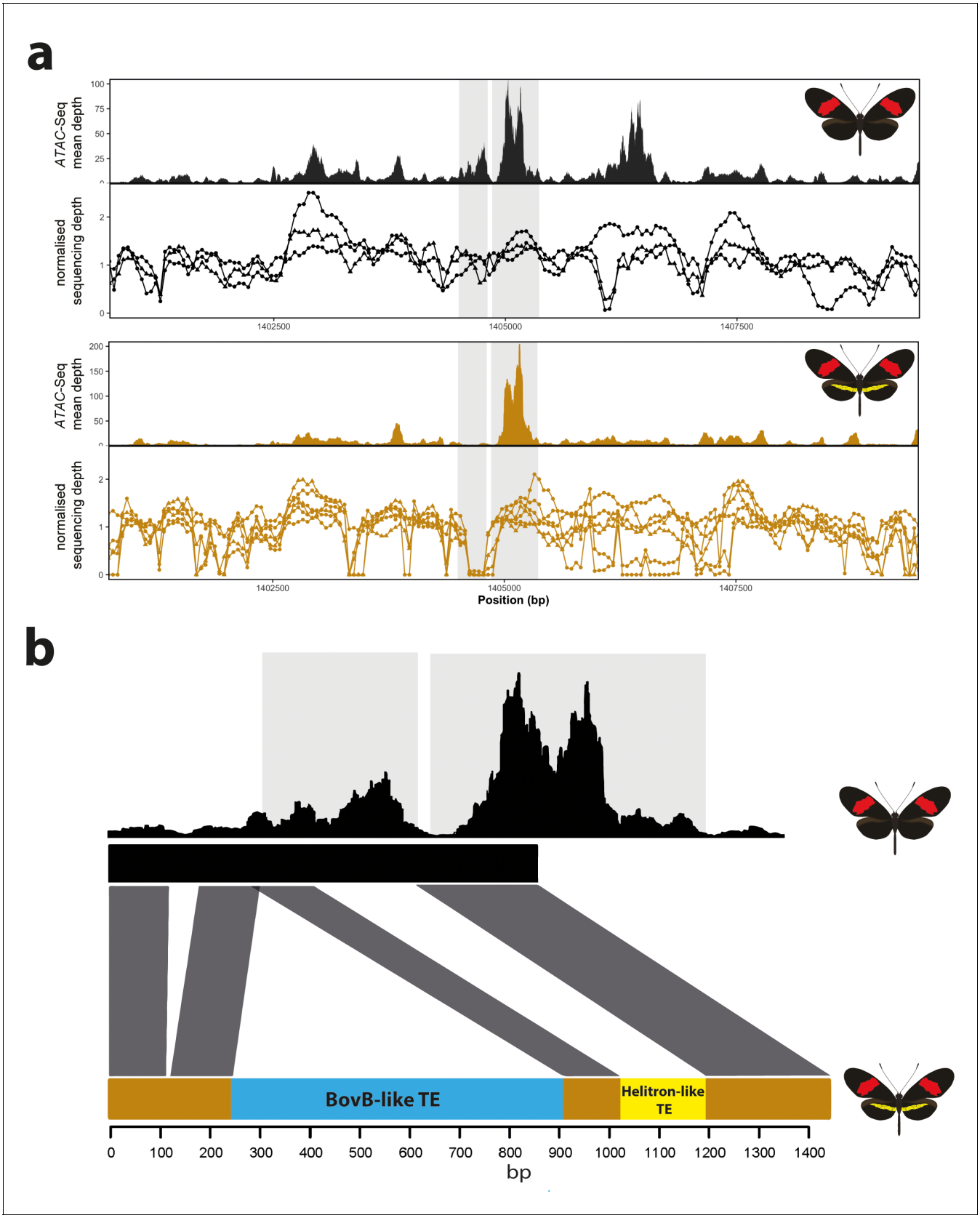

Figure 8. Coverage drop indicative of deletions in yellow-barred populations of *H. melpomene*. (**a**) Mean sequence depth for *ATAC-seq* traces for the excised CRE are shown above normalised depth in sequencing coverage for populations of *H.melpomene* (circles) and H. *timareta* (triangles) differing

Figure 8 continued on next page

Figure 8 continued

for the presence of a yellow bar. Yellow-barred populations display a drop in coverage for both ATAC signal and sequencing depth at a position corresponding to a portion of the targeted CRE (highlighted by the grey lines). Morphs analysed for melanic hindwing *H. melpomene* and *H. timareta: H. m. maletti*, *H. m. melpomene*, *H. t. florencia*. Morphs analysed for yellow-barred *H. melpomene* and *H. timareta: H. m. bellula, H. m. amaryllis, H. m. rosina, H. m. burchelli, H t. thelxione, H. t. tristero*. (**b**) Sanger sequencing of target regions in *H. m. melpomene* and *H. m. rosina* reveals an insertion of two TE elements surrounding the yellow bar CRE. A larger BovB-like element of 690 bp (blue) and a smaller 163 bp Helitron-like element (yellow) are present in the *H. m. rosina* sequences, but not the *H. m. melpomene* sequences. Base pair positions of the consensus Sanger sequencing traces are shown below.

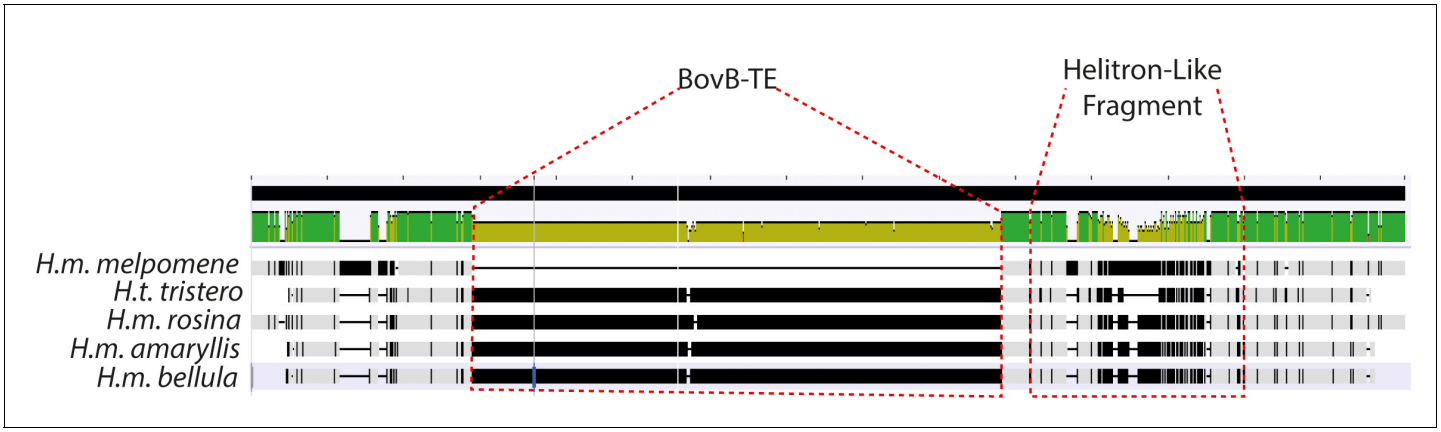

Figure 8—figure supplement 1. Alignment visualisation of the sequences above. The BovB-TE insertion is evident in all yellow-barred morphs, as well as the divergent Helitron-like sequence. This is absent from the black hindwing morph (top, *H.m. melpomene*).

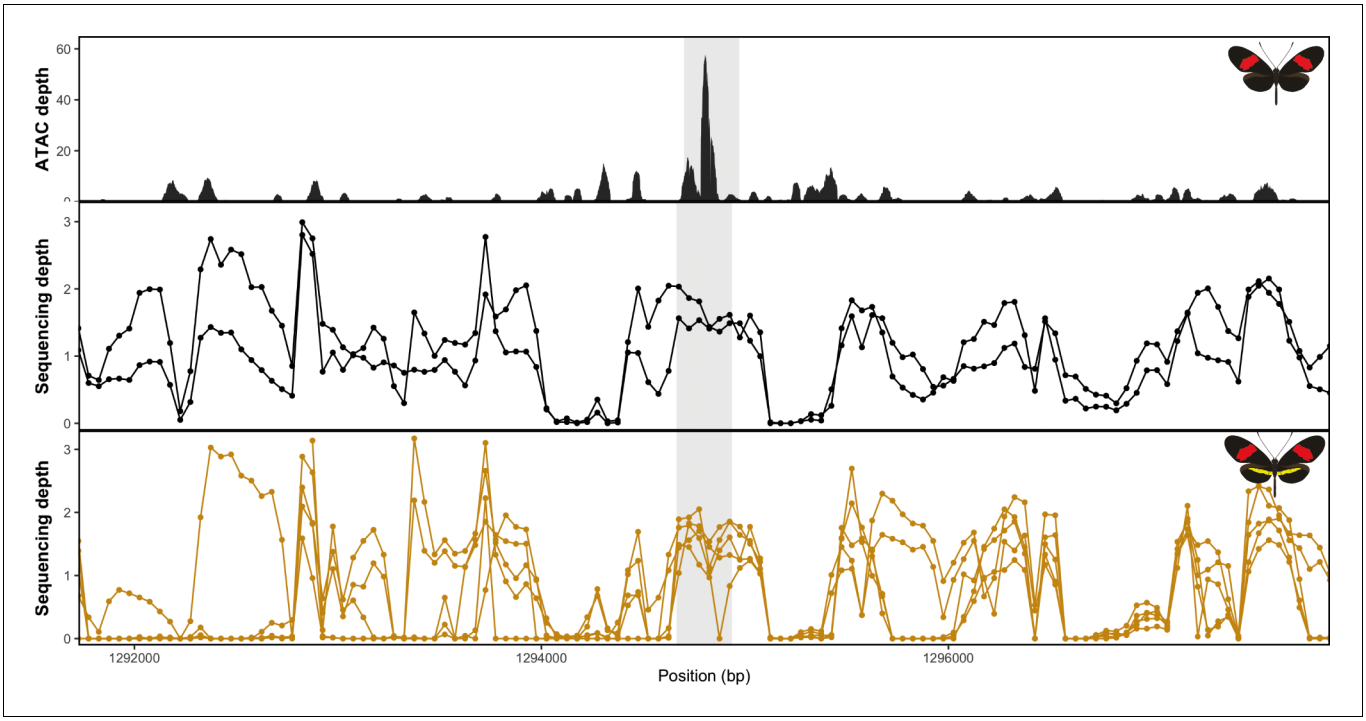

Figure 8—figure supplement 2. No evidence of deletion at the yellow bar CRE in *H. erato* populations. Mean sequence depth for *ATAC-Seq* in *H. erato* (top) and normalised sequencing depth for black hindwing populations (middle) and yellow-barred populations (bottom). Sequences were mapped against the *H. erato lativitta* reference.

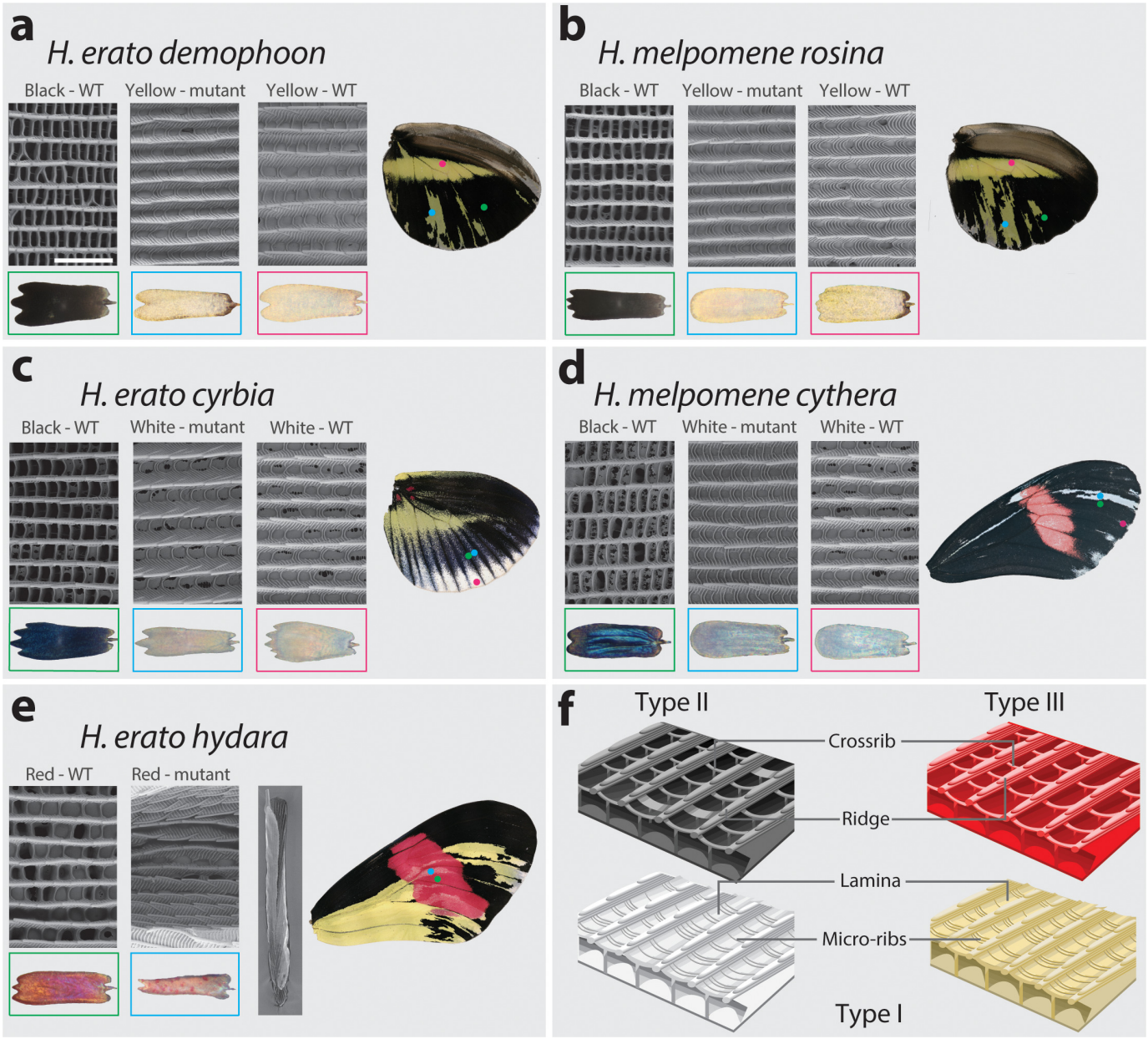

Figure 9. SEM reveals structural changes induced by *cortex* KO. Ultrastructural morphology of *H. erato demophoon* (**a**) and *H. melpomene rosina* (**b**) hindwing scales for wild-type (WT) black, mutant yellow and wild-type yellow scales. Light micrographs of each scale are shown below the representative SEM images. Scale morphologies are also presented for morphs displaying shifts to white scales in *H. erato cyrbia* (**c**) and *H. melpomene cythera* (**d**). Structural changes in the red scales of *H. erato hydara* (**e**) are accompanied by scale deformations, resulting in a curled appearance. Cartoon depiction of scale ultrastructure illustrating differences between scale types (**f**). Type I scales are characterised by the presence of a lamina covering the scale windows and by microribs joining the longitudinal ridges. Type II scale cells display larger crossribs and lack a lamina covering the scale windows. Type III scale cells and are characterised by larger spacing between crossribs and ridges. Scale bar in (**a**) = 3 µm.

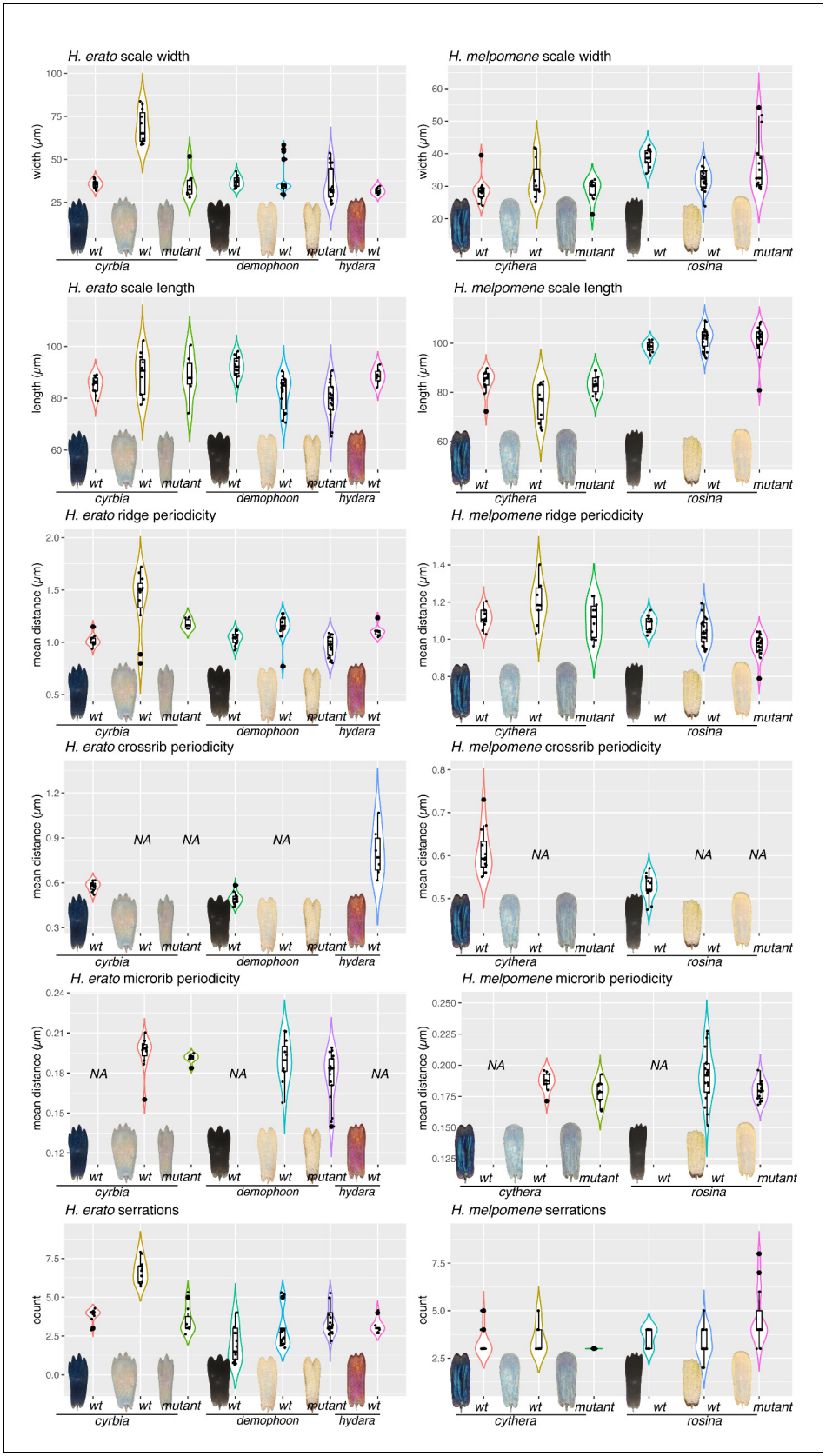

Figure 9—figure supplement 1. Quantitative measures of scale structures and features. For each scale type depicted in ***Figure 9***, between 8 and 15 scales were removed from the wing with an eyelash tool and imaged on SEM at 3000×. (Raw EM stitches can be found at the Dryad entry for this

Figure 9—figure supplement 1 continued on next page

Figure 9—figure supplement 1 continued

manuscript.) Each measurement was taken as previously described by ***Day et al., 2019***. Briefly, a line segment was drawn over the scale in FIJI, and pixel intensity levels extracted. The resulting curves were subject to Fourier analysis to get mean measures for Ridge periodicity, crossrib periodicity and microrib periodicity. Serrations were counted manually.

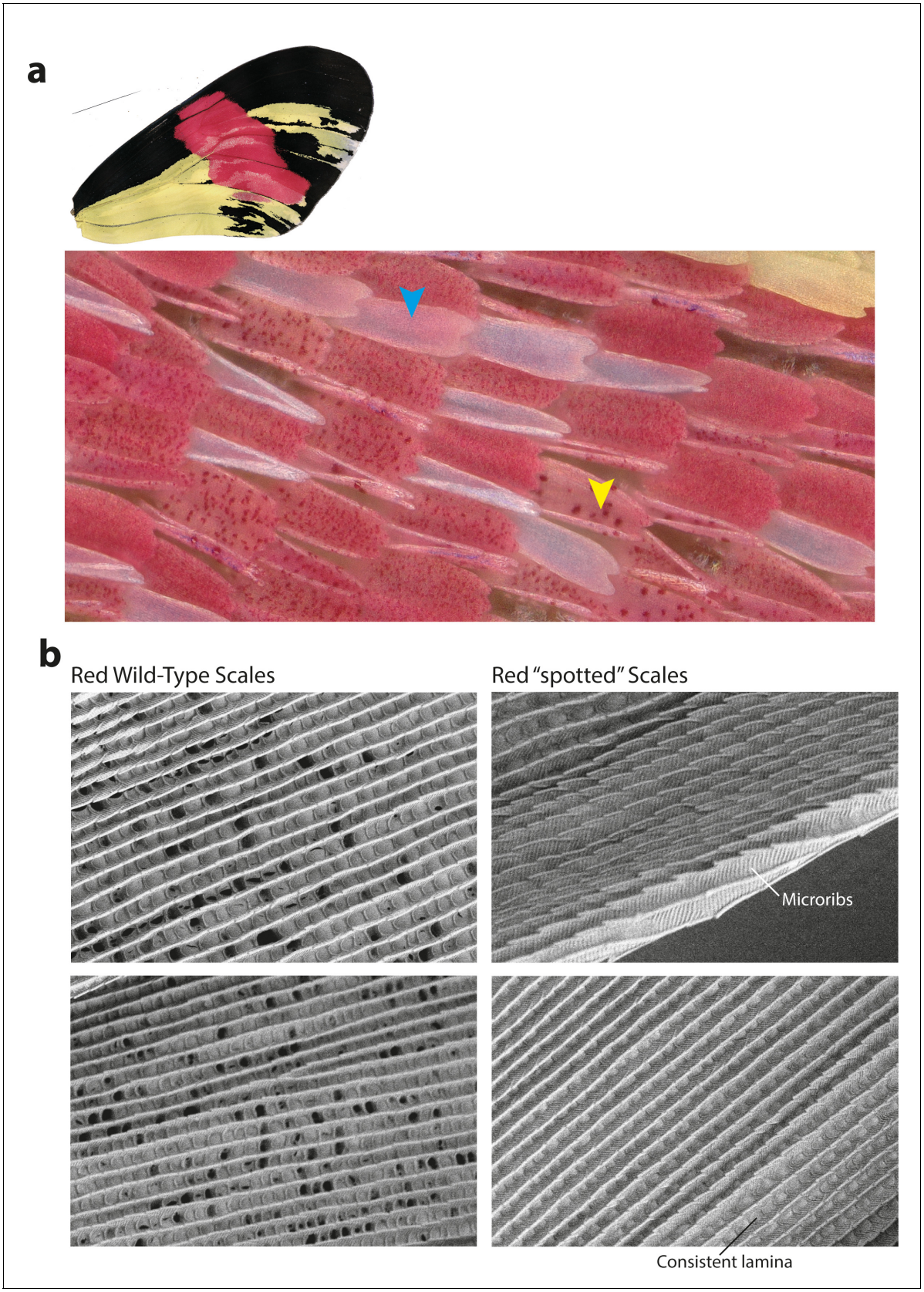

Figure 9—figure supplement 2. *Cortex* KOs in red scales produce aberrant morphologies with features consistent with Type I scale transformations. (**a**) *Cortex* perturbations result in both fully white scales across the red band (blue arrowhead) as well as a 'spotted' phenotype, where the pigment

Figure 9—figure supplement 2 continued on next page

Figure 9—figure supplement 2 continued

appears to be asymmetrically deposited across the scale (yellow arrowhead). Many of the mutant scales also take up an aberrant morphology and appear curled in shape. (**b**) SEM images reveal that the mutated scales have features consistent with Type-I-like morphology, including the presence of microribs and consistent lamina covering the scale windows.

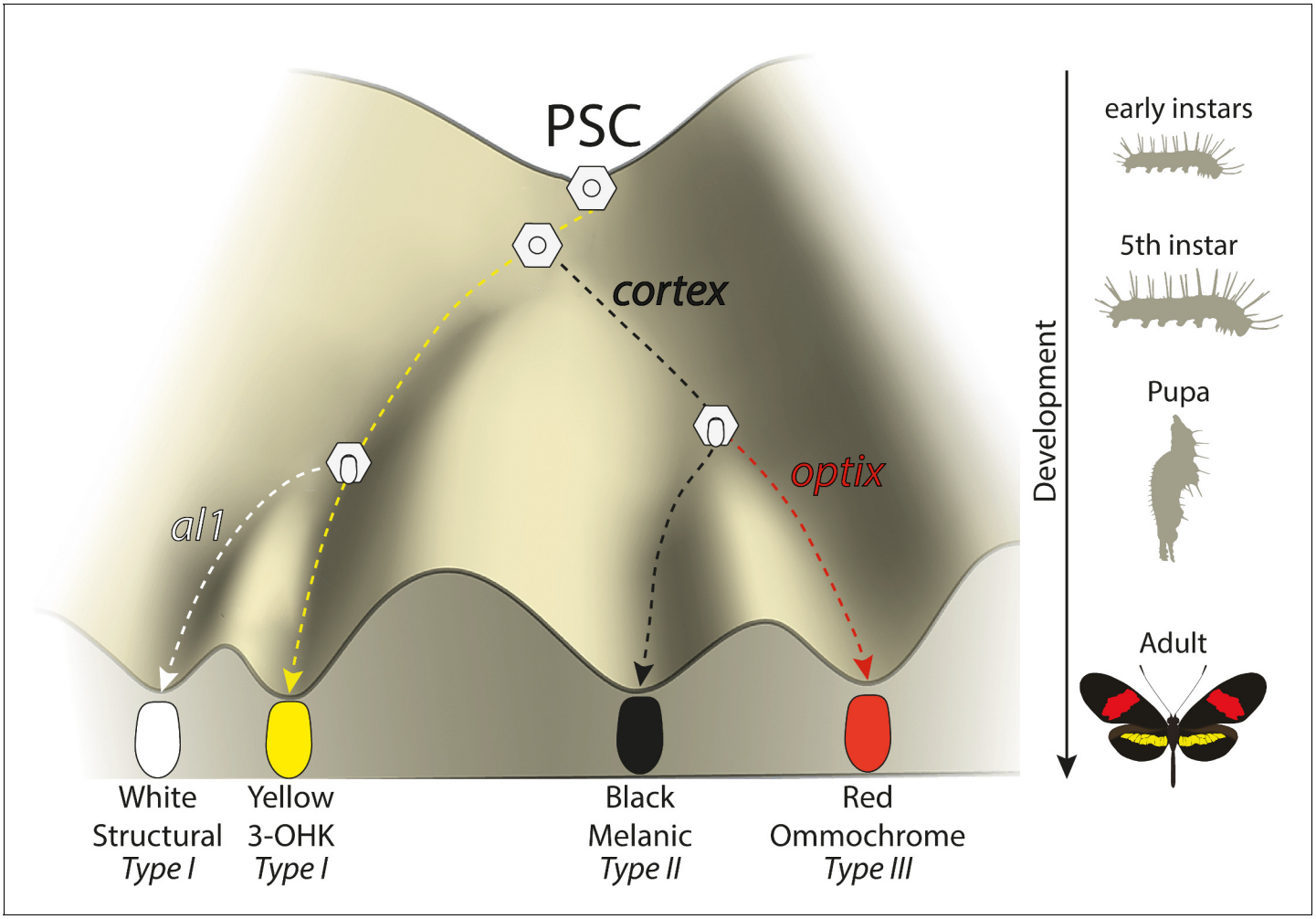

Figure 10. Expression of key genes affect scale fate decisions and influence downstream pigmentation state. During early-instar development, wing disc cells differentiate into presumptive scale cells (PSCs). Throughout fifth-instar growth, PSCs express key scale cell specification genes such as *cortex*, which induce differentiation into Type II (*optix*–) scales or Type III (*optix*+) scales. In the absence of *cortex*, scale cells differentiate into Type I scales, which differ in pigmentation state based on 3-OHK synthesis controlled by *aristaless1* expression. Model based on the epigenetic landscape (Waddington) and by observations made by ***Gilbert et al., 1987***.